

# Multidecadal analysis of Lake Garda water balance

Luigi Hinegk,<sup>1</sup> Luca Adami,<sup>1\*</sup> Sebastiano Piccolroaz,<sup>1</sup> Marina Amadori,<sup>1,2</sup> Marcello Moretti,<sup>3</sup> Marco Tubino,<sup>1</sup> Marco Toffolon<sup>1</sup>

<sup>1</sup>Department of Civil, Environmental and Mechanical Engineering (DICAM), University of Trento, Via Mesiano 77, 28122 Trento;

<sup>2</sup>Institute for Electromagnetic Sensing of the Environment, National Research Council, Via Corti 12, 20133, Milan; <sup>3</sup>Interregional Agency for the Po River (AIPo), Vicolo Canove 26, Mantova, Italy

## ABSTRACT

Lake Garda, the largest in Italy, is a major source of water supply inserted in a trans-regional area, sustaining an ever-increasing variety of water interests since the XX century. We perform a multidecadal (1928-2020) water balance, estimating the long-term evolution of the input and output components under changing anthropogenic and climatic stressors. First, we present our hydrometeorological database, assembled through consistent collection and digitization of data from different sources. Then, we analyse the annual water balance, assessing the magnitude of the residual term, i.e., the unknown term that embeds uncertainties and potential sources of error, closing the water balance equation. Uncertainties are investigated by applying a multi-method analysis for over-lake evaporation and catchment evapotranspiration. Land use evolution, contributions from the Mount Baldo area as well as the potential role of groundwater fluxes are additionally analysed. Eventually, we compute a sensitivity analysis to delineate the role of each component on the lake's level and outflow variations. The long-term analysis allows for distinguishing some trends in the input and output components of the water balance. Differences emerged in the periods before and after the lake's impoundment (1951), and some effects of climate modifications appeared in the last decades. Precipitation over the catchment has a major influence on the water availability within the catchment, a result confirmed by the sensitivity analysis. The entity of the residual term, which represents the unaccounted contributions,

calls into question the role of the groundwater fluxes and the time scale of the analysis. The multi-method analysis highlights the dependency of the different lake evaporation and catchment evapotranspiration methods on the amount of data available.

Corresponding author: luca.adami@unitn.it

Key words: limnology; water resources; long-term trends; historical analysis; long-term water budget; multi-method analysis.

Citation: Hinegk L, Adami L, Piccolroaz S, Amadori M, Moretti M, Tubino M, Toffolon M. Multidecadal analysis of Lake Garda water balance. *J. Limnol.* 2023;82:2144.

Edited by: Michela Rogora, National Research Council, Water Research Institute (CNR-IRSA), Verbania Pallanza, Italy.

Contributions: LH, LA, SB, MA, MT, MTo, involved in planning and supervised the work; LH, LA, processed the experimental data, performed the analysis and designed the figures; LH, LA, MA, SB, drafted the manuscript; SB, performed the calculations with air2water model; MT, MTo, MM, aided in interpreting the results and worked on the manuscript. All authors discussed the results and commented on the manuscript, read and approved the final version of the manuscript and agreed to be accountable for all aspects of the work.

Received: 16 May 2023.

Accepted: 30 September 2023.

Publisher's note: all claims expressed in this article are solely those of the authors and do not necessarily represent those of their affiliated organizations, or those of the publisher, the editors and the reviewers. Any product that may be evaluated in this article or claim that may be made by its manufacturer is not guaranteed or endorsed by the publisher.

©Copyright: the Author(s), 2023

Licensee PAGEPress, Italy

*J. Limnol.*, 2023; 82:2144

DOI: 10.4081/jlimnol.2023.2144

This work is licensed under a Creative Commons Attribution-NonCommercial 4.0 International License (CC BY-NC 4.0).

## INTRODUCTION

The accurate closure of the water balance of a lake is often a challenge for managers and practitioners who are asked to preserve the value of lakes as water resources. Lake water balance analysis is extremely useful to reveal climate change effects (Szesztay, 1974; Adrian *et al.*, 2009; Schulz *et al.*, 2020), water quality deterioration at different spatio-temporal scales (Gibson *et al.*, 2006; Li *et al.*, 2007; Chebud and Melesse, 2009; Guo *et al.*, 2015), and can shed light on the hydroclimatic factors mostly influencing the annual and seasonal water availability and use. Furthermore, long-term water balance studies can promote adaptive strategies for meeting current and projected human and environmental needs (Fowe *et al.*, 2015; Gronewold *et al.*, 2020), and planning restoration projects (Lerman and Hull, 1987; Jeppesen *et al.*, 2009).

Nevertheless, even the simplest computation of the lake water balance equation (water inputs equal water outputs and storage variation) is affected by biases and uncertainties. If such inaccuracies are not properly considered, relevant errors and wrong conclusions can be reached, possibly leading to ineffective solutions for water management policies. In this regard, Winter (1981) reviewed 23 water balance studies on lakes in the United States and listed several sources of uncertainties, including factors related to density and location of the available gauging stations, data processing (temporal averaging and calculation of the components of the water balance) and

interpretation of the results. In data-based analyses, the appropriate quantification of the different lake water balance terms (*e.g.*, over-lake precipitation and evaporation, surface and subsurface fluxes) depends on the quantity and reliability of the available data recorded at the existing gauging stations, which in turn depends on the study area as well as on the time window considered. In addition, inappropriate assumptions, over-simplifications and over-parameterizations of the models used to quantify some lake water balance terms (*e.g.*, evaporation) further contribute to the final (inevitable) uncertainty. Overall, the various factors listed above compose the so-called "epistemic" uncertainty that eventually propagates the errors within the computation (Efstratiadis and Koutsoyiannis, 2010).

Aimed at quantifying to what degree different models used to compute the different water balance components contribute to the overall uncertainty, several comparative studies investigated alternative methods for the estimation of *e.g.*, evaporation and evapotranspiration. A large number of comparative studies analysed the accuracy of over-lake evaporation methods (Rosenberry *et al.*, 2007; Elsawwaf *et al.*, 2010) by considering the local availability of data (Rimmer *et al.*, 2009; Majidi *et al.*, 2015), the temporal scales analysed (Winter *et al.*, 2003; Lowe *et al.*, 2009) and the influence of climatic factors (Yin and Nicholson, 1998; Lenters *et al.*, 2005). As for evapotranspiration, such component is often included in rainfall-runoff models to estimate the streamflow contribution from ungauged catchments of a lake (Zhao *et al.*, 2013; Birhanu *et al.*, 2018) and it has been studied extensively, with various methods available (Lu *et al.*, 2005; Ravazzani *et al.*, 2012; McMahon *et al.*, 2013).

A common practice in water balance analyses is to embed all the uncertainties and potential sources of error into a residual component ( $X$ ) that closes the lake water balance equation. In many cases, this approach provided important insights into the existence of some neglected water input or output terms (Wale *et al.*, 2009; Zhou *et al.*, 2013). However, a small value of  $X$  does not necessarily indicate a high computation accuracy, as biases associated with the other components can offset each other (Safeeq *et al.*, 2021). Yet, the  $X$  term remains a valid indicator of the reliability of the assumptions made, and such reliability can be strengthened by adopting more than one method to estimate the components of the water balance.

In this study, we compute 84 years of water balance of Lake Garda, divided into two periods (1928-1941 and 1951-2020). Lake Garda is the largest lake in Italy and represents a major source for water supply (Berbenni *et al.*, 1992; Goffi *et al.*, 2021) for 42 municipalities located in two separate regions (Lombardy, Veneto) and one province (Autonomous Province of Trento). Over the last decades, the administrative fragmentation of such inter-

regional context entailed a long-term issue for the fair distribution of water among the contrasting and ever-growing water needs (Berbenni *et al.*, 1992). The first systematic water balance of Lake Garda was carried out over the period 1921-1960 (Berbenni *et al.*, 1992) and the residual unresolved term was mainly attributed to the neglected input of groundwater fluxes, with an estimated average value of  $7 \text{ m}^3 \text{ s}^{-1}$ . More recently, Longinelli *et al.* (2008) computed a 9-year (1998-2006) balance of Lake Garda based on an isotope study, from which large imbalances appeared, *i.e.*, the lake total inflows resulted in approximately half of the lake outflows, confirming the relevant role played by the deep aquifers of the area. Thus, despite the strategic importance of Lake Garda water resource, there is still a lack of an up-to-date understanding of the hydrogeological and climatic factors that control the lake water balance and have influenced it over the last century.

In our multidecadal lake water balance, we investigate the long-term variations of the different inputs and outputs to assess the main drivers of the water availability within the catchment over a long period (1928-2020). Concurrently, we perform up to 20 possible versions of the lake water balance equation by implementing methods to estimate over-lake evaporation and catchment evapotranspiration requiring different quantities and types of data. By comparing different data-demanding methods, from the simplest to the most advanced, an estimate of the uncertainties and robustness of each configuration is possible. We note that such multi-model approach is increasingly adopted in the limnological community (Scavia *et al.*, 2016; Moore *et al.*, 2021; Golub *et al.*, 2022). In fact, a critical cost-performance analysis of different models particularly helps in data-limited contexts or when the amount and type of hydroclimatic observations change over the years of historical time series.

The main objectives of the paper can be described as follows: i) to estimate the long-term evolution of the input and output components of Lake Garda water balance at an annual time scale; ii) to build a consistent long-term hydrometeorological database from different sources in order to compute an accurate water balance; iii) to analyze the annual water balance of the lake, and the magnitude of the uncertainties.

In the following sections, we first analyse the standard hydroclimatic observations used in this study. An insight on the spatio-temporal distribution of the data collected is provided, with a specific focus on the datasets of air temperature and precipitation. Then, we present the annual water balance of Lake Garda over the periods 1928-1941 and 1951-2020 to investigate the major drivers of water availability within the lake catchment and to quantify the residual term  $X$  throughout the years. We

discuss how the presented results are affected by different over-lake evaporation and catchment evapotranspiration models. We also examine the possible role played on the overall water budget by the groundwater fluxes, by the contributions from the Mount Baldo area (which is not included in the surface drainage area of the lake, but might contribute through the aquifer), and by the land use evolution. Eventually, we perform a sensitivity analysis to explore the factors that have mainly controlled the Lake Garda water level and outflow, assessing the impact of possible uncertainties in the estimate of some water balance components (*e.g.*, precipitation, evaporation). This final analysis is of primary interest in view of the multiple water needs and stakes that characterize the downstream Mincio River catchment.

## METHODS

### Study area

Lake Garda (Fig. 1) ranks first in inland freshwater bodies of Italy for water volume (49 km<sup>3</sup>) and surface area (368 km<sup>2</sup>). The lake is located at the foot of the Alps, a nationally relevant region for the environmental and economic importance of its water resources. The Lake Garda catchment is inserted in a typically Alpine climate, with air temperature and precipitation variability influenced by the Mediterranean Sea (Brugnara and Maugeri, 2019). The main hydromorphological characteristics of the lake are listed in Tab. 1. The lake level is monitored daily at the closure of the catchment (2290 km<sup>2</sup>) on the southernmost

**Tab. 1.** Hydromorphological characteristics of Lake Garda. The extension of the catchment considered in the analysis is shown in Fig. 1.

Altitude*	(m asl)	65	Width*	(km)	17
Average depth*	(m)	133	Gauging station reference level#	(m asl)	64.03
Maximum depth*	(m)	350	Average water level# (1951-2020)	(m asl)	65.43
Surface area*	(km <sup>2</sup> )	368	Average surface outflow# (1951-2020)	(m <sup>3</sup> s <sup>-1</sup> )	53
Catchment area*	(km <sup>2</sup> )	2290	Average surface inflow° (2008-2018)	(m <sup>3</sup> s <sup>-1</sup> )	35
Shore length	(km)	158	Theoretical retention time#	(year)	30
Surface area per catchment area ratio#	(%)	16	Origin*		glacial
Volume*	(km <sup>3</sup> )	49	Mixing regime*		oligomictic
Length*	(km)	52	Trophic status*		oligo-mesotrophic

\*Tolotti *et al.* (2018); #Hinegk *et al.* (2022); °Provincial Agency for water resources and energy of Trento (APRIE, <http://www.energia.provincia.tn.it/>).

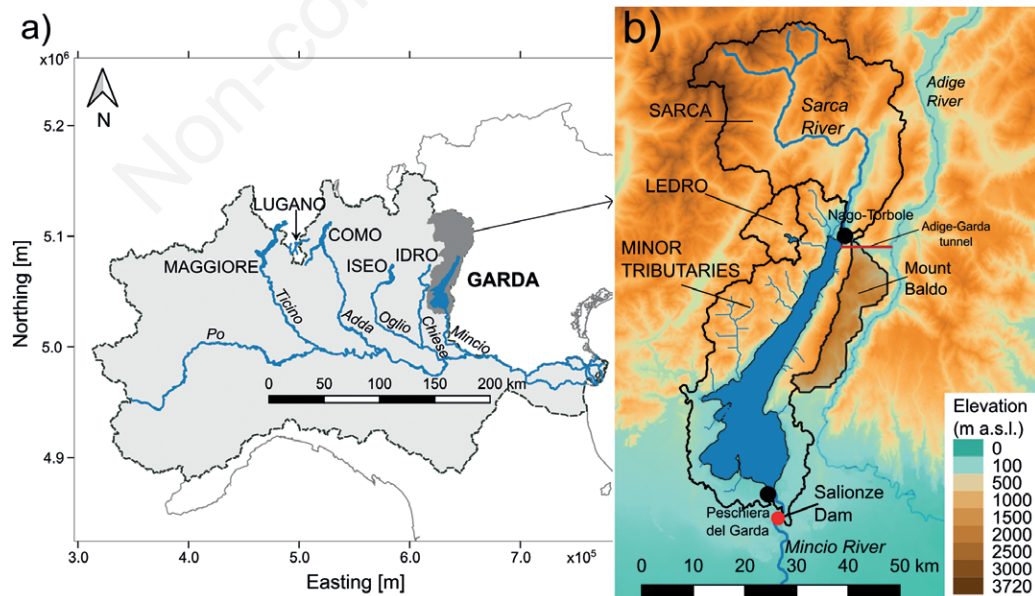


**Fig. 1.** a) Location of Lake Garda and its catchment in the framework of the deep Italian subalpine lakes. b) Focus on the Sarca-Garda system, which includes the Sarca (main tributary) catchment, the Ledro catchment, the minor tributaries catchment and the Mount Baldo catchment. The regulation system of the lake is indicated by a red dot (Salionze Dam). The red line connecting the Adige River and Lake Garda outlines the Adige Garda tunnel layout.

shore, in the municipality of Peschiera del Garda, where the lake waters flow through a confined watercourse (N-S direction) for 5 km before reaching the Salionze Dam in the municipality of Ponti sul Mincio (catchment 2350 km<sup>2</sup>). This infrastructure regulates the outflow regime of the lake through three distinct channels, *i.e.*, the Mincio River and the two irrigation-hydropower artificial channels named Virgilio and Seriola-Prevaldesca. The Salionze Dam was completed in 1951 to primarily accomplish the main water needs of the downstream Mincio River catchment, *i.e.*, flood protection and irrigation demands.

The regulation of Lake Garda is the result of more than a century of discussions and projects, *e.g.*, the work of Martinelli (1881) in the XIX century. With the advent of the XX century, the regulation of the Lake Garda level and outflow become an increasingly relevant issue, with several notes and studies, including those drawn up Eng. Poletta in 1903 (followed by others) until the final approval of the executive project of Eng. Silvestri in 1938 (Togliani, 2014). Other important works in the process were carried out by De Marchi (1919, 1920). Nevertheless, ever-growing water requirements have contributed to drastic changes in the long-term trend as well as the seasonal behaviour of both water levels and outflows after lake regulation (Hinegk *et al.*, 2022).

The Sarca River represents the main tributary, flowing from the Presanella mountain to the municipality of Nago-Torbole (65 m asl), where the river reaches the northernmost shore of the lake. The pristine nivo-glacial flow regime of the Sarca River has been heavily altered since the beginning of the XX century through the construction of a complex system of artificial waterways to support the growing hydropower production in the area (Carolli *et al.*, 2021), determining lower flow conditions in summer season and higher flow conditions during winter (Berbenni *et al.*, 1992). In fact, the numerous hydropower plants including the one located just 3 km upstream of the Sarca River's mouth (Torbole hydropower plant) have affected the annual cycle of the Sarca River regime without modifying the total volume released to Lake Garda. In addition to the Sarca River, more than 20 ungauged tributaries (among which the Ponale River from the Ledro catchment) flow into the lake from the eastern and western shores, likely representing a non-negligible contribution to the water balance. In this work, we define as Lake Garda catchment the overall contributing catchment, *i.e.*, the sum of the catchments related to the Sarca River, the Ponale River and the minor ungauged tributaries.

The Adige-Garda diversion tunnel occasionally influences the lake level variation, with minor effects in terms of annual water balance according to Berbenni *et al.* (1992). Such tunnel is a 10 km-long interbasin water transfer system that can convey up to 500 m<sup>3</sup>s<sup>-1</sup> from the Adige River to Lake Garda in case of extreme flood events

(Fig. 1b). Its role has been considered for all major floods (*i.e.*, registered volume greater than 4 Mm<sup>3</sup>), while annual opening operations for technical maintenance have been neglected.

Lastly, the eastern part of the Mount Baldo catchment (grey shaded area in Fig. 1b), located along the eastern shore of the lake, potentially contributes to the Lake Garda water balance, although topographically not belonging to the lake watershed. Indeed, it is characterized by dip slope structures plunging into Lake Garda and by calcareous, chalky and dolomitic rocks which may promote water conveyance to the lake (Zorzin and Tottola, 2020).

### Data collection and processing

The multi-regional context of Lake Garda required the collection of hydro-meteorological observations from different agencies. Such effort implied the exploitation of both public online sources and historical hand-written documents. Data from the first half of the XX century (*i.e.*, lake levels, lake outflows, precipitation and maximum and minimum air temperature) were digitized by hand starting from the Italian Annual Hydrological Books provided by the Italian Hydrological Service (Ministero dei Lavori Pubblici - Servizio Idrografico, 1917). Data from the second half of the XX century were downloaded from the online portals of the Autonomous Province of Trento (<https://www.meteotrentino.it>) and Bolzano (<https://meteo.provincia.bz.it>) and of the Regional Agencies for the Environmental Protection of Lombardia (ARPA Lombardia, <https://idro.arpalombardia.it>, <https://www.arpalombardia.it>) and Veneto (ARPAV, <https://www.arpa.veneto.it>). Additional data were provided upon request by ARPAV. The resulting database represents a unique source of hydro-meteorological data from the XX century for Lake Garda and is a comprehensive, site-specific and systematic baseline of data for this inter-regional context.

Fig. 2 summarizes the data availability over time and space in the case study. The water balance was performed for those time periods covered by a sufficient availability of Lake Garda water levels, outflows, as well as precipitation and air temperature (light blue shaded areas in Fig. 2 a,b), which represent the essential meteorological variables for the water balance computation. Accordingly, the period 1942-1950 was discarded due to the absence or scarcity of some relevant data, caused by the advent and aftermath of World War II in Italy (Brugnara *et al.*, 2012). Thus, we analyzed two periods, *i.e.*, 1928-1941 and 1951-2020, for a total of 84 years. The selected time series are representative of the pre-regulated and post-regulated regime of Lake Garda, due to the Salionze dam building in 1951.

In general, precipitation data are more abundant than air temperature data (197 against 151 gauging stations over the whole period of study, respectively).

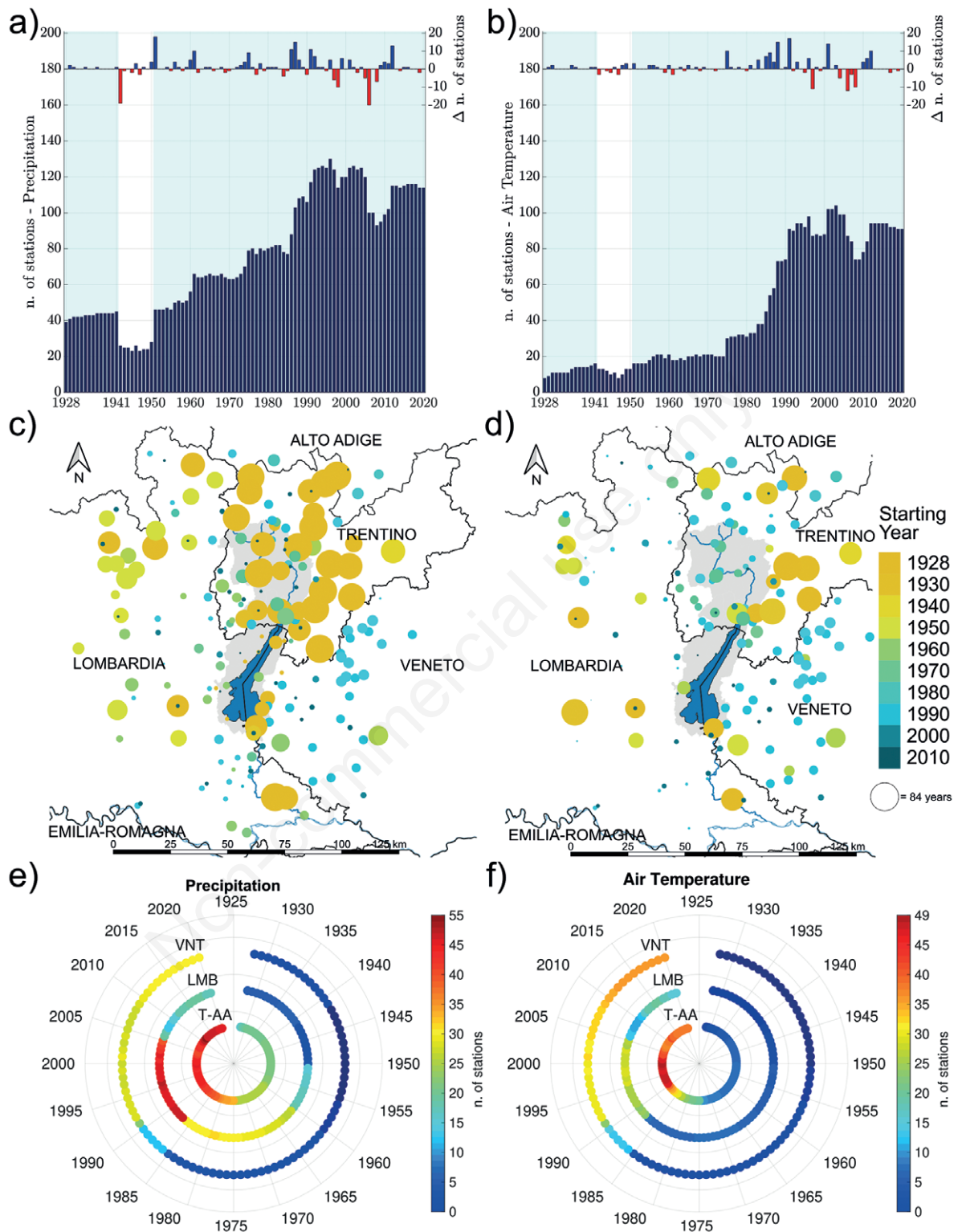


**Fig. 2.** a,b) Number of rainfall (a) and air temperature (b) stations operative in each year from 1928 to 2020 (dark blue bars at the bottom of the plots) and their variation throughout the years (red and blue bars at the top); light blue shaded areas indicate the periods taken for the water balance analysis. c,d) Location of the rainfall (c) and air temperature (d) stations inside and surrounding the Sarca-Garda catchment (grey shaded area); the colour and size of each marker is related to the starting year of observations and the number of years with available data respectively. e,f) Number of rainfall (e) and air temperature (f) stations with available data based on the region. VNT, Veneto; LMB, Lombardy; T-AA, Trentino Alto-Adige.

The availability of data increased over the years, in particular starting from 1990 in all regions, with the exception of the period 2005-2010 when some obsolete gauging stations were dismissed (Fig. 2 a,b). In terms of spatial distribution (Fig. 2 c,d) the stations are homogeneously distributed but show a small asymmetry towards the Province of Trento, particularly in recent decades (Fig. 2 e,f).

Data on lake outflow and water level are available for the whole considered period, and were collected reaching back the 1888 in a recent study (Hinegk *et al.*, 2022). Data of lake's inflows are available only for the main tributary, *i.e.*, the Sarca River, and limited to 1954-1960 and 2008-2017. Thus, the collected precipitation and air temperature data, particularly within the Trentino-Alto Adige region, were essential to estimate the inflows for the lacking years of the Sarca River as well as for the other minor tributaries for the lacking years. Moreover, in the upper part of the Sarca catchment three main group glaciers are present (namely Adamello, Presanella and Brenta). Their role in the annual balance has been estimated to provide an additional contribution in terms of precipitation equivalence, *e.g.*, for Adamello glacier estimated in 1290 mm of water equivalent in the period 1995-2006 (Ranzi *et al.*, 2010), with an acceleration of the annual contribution starting from the 80s (Santilli *et al.*, 2002; Baroni and Carton, 1990; Calmanti *et al.* 2007). This effect has been estimated in the Sarca catchment through the analysis of two available DTM in the Sarca catchments (years 1984 and 2003) with a resolution of 10 m, we estimated the ice volume lost by glaciers and converted in an average annual discharge due to ice melt, using an ice density equal to 900 kg/m<sup>3</sup> for the conversion ice-water (Ranzi *et al.*, 2019; Freudiger *et al.*, 2021). We found that this estimate discharge for the Sarca catchment is 0.84 m<sup>3</sup>/s, that represents nearly 2.4.% of the total average discharge of the Sarca basin in the period 2008-2018 (about 35.7 m<sup>3</sup>/s) and 1.9% of the average total inflow of the Sarca-Garda catchment (43.7 m<sup>3</sup>/s) considering the same time interval. The mean thickness change of ice for the Sarca catchment is -0.41 m/year. A comparable result has been found by D'agata *et al.* 2018 in the Adda catchment (-0.57 m/year in the period 1981-2007), contiguous to the Sarca basin to the west. Although this component has not been directly included in eq. 1, its effect can be considered negligible in a first approximation.

A gridded-dataset of precipitation and evapotranspiration was constructed through the application of the kriging method (Goovaerts *et al.*, 1997), additionally including gauging stations located beyond the grid borders to ensure reliable results. We adopted a 500m x 500m grid to fairly represent the catchment as well as the lake coastline (see Fig. S4). Besides the lake surface area, we included the Sarca, Ledro and minor tributaries catchments

(Fig. 1b), estimating the spatial patterns of the precipitation and evapotranspiration components. We compared the Ordinary Kriging (OK) and Kriging with External Drift (KED) methods, selecting the best interpolation technique through the Leave One Out Cross Validation procedure. Details of the kriging techniques are summarised in Appendix (see Kriging methods for spatial interpolation), where the discretization grid and the average spatial distribution of precipitation and mean air temperature are also shown. The gridded-dataset of precipitation for the lake area was used to quantify the over-lake precipitation directly contributing to the lake water balance. The gridded-dataset of both precipitation and evapotranspiration for the contributing catchments was instead used to determine the inflow contributions of the Sarca River and of the other ungauged streams by implementing a simple hydrological balance (see section "Estimation of inflows"). For the Sarca River, the daily data available for the period 2008-2017 allowed for an ad hoc calibration of the simple hydrological balance adopted.

### Lake water balance equation

The lake water balance was computed on an annual time scale, according to the hydrological year, *i.e.*, from October 1<sup>st</sup> to September 30<sup>th</sup>, to properly consider snow melt and snow accumulation periods. We assumed the beginning of October as the end of the possible contribution of ice and snow-melted water from the Lake Garda catchment. In this way, the annual net precipitation (including snow) can be transformed, as a first approximation, into annual inflows to the lake without significant delay effects. Considering the annual time scale, we also assumed that the whole net rainfall (*i.e.*, P-ET<sub>a</sub>) contributes to the water balance, either in surface waters or in subsurface waters, within a year. This is a strong simplification in the computation of the water balance, although an acceptable way to deal with the large uncertainties in setting up such a long-term analysis. The approximation is strictly related to the choice of annual time scale and it is not valid at shorter time scales (daily, monthly).

Therefore, the annual water balance was expressed using annually aggregated values (calculated based on the available daily values) in the form:

$$\frac{\Delta V}{\Delta t} - (P_L + Q_i) + (EV_{L,i} + Q_{out}) - X_i = 0, \quad (\text{eq. 1})$$

where

$$\frac{\Delta V}{\Delta t} = \frac{A_L (H_{t+1} - H_t)}{\Delta t} \quad (\text{eq. 2})$$

and the index  $i = 1, \dots, n$  represents the combination of

different over-lake evaporation and evapotranspiration methods. The term  $\Delta V/\Delta t$  represents the lake volume variation over time in  $\text{m}^3/\text{s}$ , which is a function of the lake surface area  $A_L$  in  $\text{m}^2$  and of the lake levels  $H_{t+1}$  and  $H_t$  in m at time  $t+1$  and  $t$  in s, whose difference represents the annual time step  $\Delta t$ . The lake level is measured at Peschiera del Garda (Tab. 1). Over-lake precipitation and evaporation are indicated as  $P_L$  and  $EV_{L,i}$ , respectively. The term  $Q_i$  is the total ungauged water contribution conveyed from the Sarca River and the other minor tributaries, quantified according to the procedure delineated in section “Estimation of inflows” and depending on the estimate of the evapotranspiration. The term  $Q_{out}$  is the surface water outflow, represented by the total discharge released into the Mincio River. Finally, the residual term  $X$  is the unknown term that closes the water balance equation. We assume a positive value to indicate the underestimation of the total water inputs (or the overestimation of the total water outputs) and a negative value to indicate the overestimation of the total water inputs (or the underestimation of the total water outputs).

To assess the uncertainties related to the water balance, we computed a number  $n=20$  of combinations of the lake water balance (eq. 1), considering 5 over-lake evaporation ( $EV_{L,i}$ ) and 4 reference evapotranspiration (used to estimate  $Q_i$ ) methods. In this way, we explored the variation of the residual term  $X$  in response to the different methods adopted to identify which combination provides the minimum value over the entire time series.

As additional variations of the approach, we investigated the role of the Mount Baldo catchment, as well as the effect of land use changes provided by the available datasets (discussed in the section “Discussion”).

### Over-lake evaporation and catchment evapotranspiration estimates

The literature presents several methods to estimate over-lake evaporation and catchment reference evapotranspira-

tion. We decided to test 5 models to compute evaporation and 4 for evapotranspiration. All selected formulas have been widely used in the literature and mainly differ for the type (e.g., meteorological, topographic) and number (from two up to five) of input variables required. This allows comparing the different estimates depending on data availability. In addition, as the selected methods were conceived for either general or site-specific contexts, we discuss their appropriateness for our case study. The inputs required to compute the over-lake evaporation and reference evapotranspiration equations are fully described in Tab. 2, and the related equations are presented in the *Supplementary Material*.

In terms of over-lake evaporation ( $EV_L$ ), we implemented well-grounded approaches that are largely valid in different contexts, i.e., the combined approach of the Penman model (Penman, 1948), the Priestley-Taylor method (Priestley and Taylor, 1972), the mass transfer method of Dalton (Dalton, 1802), herein implemented as reported by Fink *et al.* (2014) and already applied to Lake Garda by Matta *et al.* 2022, the simplified Penman, (1948) method in case of no wind data proposed by Valiantzas (2006), and the Jensen and Haise (1963) method. Such methods either exclude the lake surface water temperature as an input variable (Penman, 1948; Priestley and Taylor, 1972; Jensen and Haise, 1963; Valiantzas, 2006), or include the aerodynamic component, thus requiring wind data (Penman, 1948; Fink *et al.*, 2014). The Dalton approach (Fink *et al.*, 2014) includes the lake surface water temperature (LSWT). In this study, the daily LSWT was reconstructed for Lake Garda based on air temperature by means of the air2water model (Piccolroaz *et al.*, 2013; Toffolon *et al.*, 2014; Piccolroaz, 2016). Interested readers are referred to the Appendix. For those methods requiring wind speed and relative humidity, we used the average annual cycle (daily values) computed from years of full data availability to fill the gaps of the time series. Daily extra-terrestrial radiation was instead estimated following Martin *et al.* (2018).

**Tab. 2.** Methods selected for estimating over-lake evaporation (EVL) and catchment reference evapotranspiration (ET0) and input variables they require.

	Equation name	Reference	AT	Rad	elev	RH	wind	LSWT
EV <sub>L</sub>	Penman	Pen	Penman, (1948)	✓	✓	✓	✓	✓
	Jensen-Haise	JH	Jensen and Haise (1963)	✓	✓			
	Priestley-Taylor	PT	Priestley and Taylor, (1972)	✓	✓	✓		
	Simplified Penman	Val	Valiantzas (2006)	✓	✓		✓	
	Dalton	Dal	Fink <i>et al.</i> (2014)	✓			✓	✓
ET <sub>0</sub>	Hargreaves-Samani	HS	Hargreaves and Samani (1985)	✓	✓			
	FAO Penman-Monteith	FAO-56 PM	Allen <i>et al.</i> (1998)	✓	✓	✓	✓	✓
	HS modified PGUAP	PGUAP	PAT (2006)	✓	✓			
	HS modified Ravazzani	HSAIp	Ravazzani <i>et al.</i> (2012)	✓	✓	✓		

AT, air temperature; Rad, radiation; elev, elevation; RH, air relative humidity; wind, wind velocity; LSWT, lake surface water temperature.

In terms of reference evapotranspiration  $ET_0$ , all implemented methods are derived from the largely adopted Hargreaves-Samani (hereafter indicated as HS, Hargreaves and Samani 1985) and FAO-56 Penman-Monteith (FAO-56 PM; Allen *et al.*, 1998) models. The FAO-56 PM method is a widely recommended version of the Penman-Monteith equation (Allen *et al.*, 1998), whereas the HS is based only on solar radiation and maximum and minimum air temperature and is largely applied in data-scarce contexts. Allen *et al.* (1998) additionally provided procedures to compute the FAO-56 PM equation in case of limited availability of data. The adoption of such simplified version of the FAO-56 PM equation is primarily suggested by Allen *et al.* (1998) before implementing the HS approach.

As the reference evapotranspiration estimates of the HS model need to be adjusted to the local conditions (Ravazzani *et al.*, 2012), we further considered two simplified models that are referred to the peri-alpine region that Lake Garda belongs to. These two methods are the HS method modified by Ravazzani *et al.* (2012) (HSAIp) and the PGUAP (Master Plan for the Utilisation of Public Waters) method of the Autonomous Province of Trento (Provincia Autonoma di Trento, 2006), both of which were conceived by adjusting the simpler HS equation by introducing correction factors determined through regression against the more data-demanding FAO-56 PM equation. On the one hand, (Ravazzani *et al.*, 2012) deal with the general inaccuracy of the original HS equation in estimating  $ET_0$  at different elevation sites by applying two calibration coefficients. On the other hand, PAT (2006) introduced a multiplication coefficient 0.7 as the result of the ratio between the HS and FAO-56 PM methods computed for those stations of the Trentino area (Fig. 1b) where the input meteorological data permitted to apply both formulations. With the exception of the HS modified model (Ravazzani *et al.*, 2012), in Tab. 2 the elevation term is adopted to estimate the atmospheric pressure as recommended by Allen *et al.* (1998). Further details are given in the *Supplementary Material*.

The actual evapotranspiration ( $ET_a$ ) depends on the land use, soil moisture and on climatic conditions. To account for this, the reference evapotranspiration ( $ET_0$ ) was first converted into the potential evapotranspiration ( $ET_p$ ) by applying the crop coefficient  $K_C$  to each cell of the catchment grid (Allen *et al.*, 1998;  $ET_p = K_C ET_0$ ), and then into the actual evapotranspiration by multiplying  $ET_p$  by a stress factor ( $\alpha$ ,  $ET_a = \alpha ET_p$ ), considering that climatic and soil conditions can further reduce the quantity of water that is actually available for evapotranspiration (Mallucci *et al.*, 2019). Since  $K_C$  depends on the land cover type, we investigated possible long-term land cover variations by referring to the annual estimations provided by the Historic Land Dynamics Assessment+ (HILDA+; Winkler *et al.*,

2021), a harmonised dataset of maps with spatial resolution of 1 km x 1 km over the period 1899-2019 (Winkler *et al.*, 2020). The land cover type of each grid cell of the domain was related to its corresponding value of  $K_C$  according to the local land use classification as reported by PAT (2006) (Tab. 3).

Starting from the  $ET_p$ , the stress factor  $\alpha$  to estimate  $ET_a$  was quantified following the procedure reported by Mallucci *et al.* (2019):

$$\alpha = \frac{\bar{P} - \bar{Q}}{\bar{ET}_p} \quad (\text{eq. 3})$$

where,  $\bar{P}$ ,  $\bar{Q}$  and  $\bar{ET}_p$  are the spatial and temporal average values over the whole period of analysis (in consistent units) of total precipitation, streamflow volume and potential evapotranspiration, respectively. We note that the computation of  $\alpha$  requires streamflow data of the catchment under analysis. Thus, we evaluated eq. 3 for the Sarca River Catchment (*i.e.*, the main tributary of Lake Garda and the only tributary for which observations are partially available) considering those years with available historical data, and then considered the value obtained as a reliable estimate also for the other drainage catchments, *i.e.*, the Ledro and minor tributaries catchments (Fig. 1b). The final value of  $\alpha$  was 0.63, comparable to the value of 0.7 estimated by Mallucci *et al.* (2019).

### Estimation of inflows

Data about the inflows provided by the catchments surrounding Lake Garda have not been recorded with proper continuity. In order to reconstruct their contribution, we assumed that the net precipitation over the lake's catchment, *i.e.*, the difference between precipitation and evapotranspiration, is a legitimate proxy of the total inflows at an annual time scale, including the sum of both surface and subsurface fluxes. In fact, on the annual basis, the large part of the water that penetrates and reaches the subsurface reservoir is expected to flow into the streams and contribute to the lake's water balance. This assumption is supported by the results of recent hydrological modeling studies realized for the Adige River Catchment, close to the region of interest and much larger, where the mean residence time of baseflow was estimated to be around 300 days (Piccolroaz *et al.*, 2015; Laiti *et al.*, 2018). Thus, the water balance for the generic catchment surrounding the lake can be written as:

$$\Delta S/\Delta t = P - ET_a + Q, \quad (\text{eq. 4})$$

Where  $\Delta S/\Delta t$  is the water stored within the generic catchment,  $P$  is the total precipitation,  $ET_a$  is the actual evapotranspiration,  $Q$  is the total discharge (*i.e.*, sum of surface and subsurface fluxes) at the closure section of the



catchment. Note that the discharge  $Q$  in this formulation represents, for the lake water balance, a component of the inflows  $Q_i$  in eq. 1).

At annual time scales, the  $\Delta S/\Delta t$  changes can be considered negligible (Budyko, 1958; Zhang *et al.*, 2008), so that eq. 4 can be simplified into:

$$Q = P - ET_a = P - \alpha ET_p \quad (\text{eq. 5})$$

which is analogous to eq. 3. The net precipitation ( $P - ET_a$ ) was therefore used as a proxy for the lake's total inflows from the surrounding catchments (Sarca River, Ledro and minor tributaries; Fig. 1b), comprising both surface and subsurface contributions.

In this way, eq. 1 can eventually be expressed as:

$$\frac{\Delta V}{\Delta t} - (P_L + P_B - ET_a) + (EV_{L,i} + Q_{out}) - X_i = 0 \quad i = 1, \dots, n \quad (\text{eq. 6})$$

Where  $P_B$  and  $ET_B$  refer to the total catchment precipitation and evapotranspiration, *i.e.*, to all the contributing catchments (Sarca, Ledro and minor tributaries).

### Sensitivity analysis

The lake level  $H$  fluctuates depending on the different components of the water balance. In the formulation of eq. 1, however,  $H$  is only present in the storage term, while it can also have an influence on the outflow  $Q_{out}$  (and, to a minor extent, on the evaporation term if the influence of the changing area is considered, an effect that is negligible in Lake Garda).

To explicitly consider the dependence of  $Q_{out}$  on  $H$ , we assumed a power-law relation between the annual means of the two variables:

$$Q_{out,k} = a_k (H - b_k)^{c_k} \quad (\text{eq. 7})$$

As this relation drastically changed after the impoundment of Lake Garda in 1951, we distinguished a natural condition ( $k=n$ ) for the pre-regulation period (1928-1941) and a regulated regime condition ( $k=r$ ) for the post-regulation (1951-2020). In eq. 7, the outflow  $Q_{out}$  is expressed in  $m^3 s^{-1}$  and the lake level  $H$  in m above the reference zero of 64.027 m asl. The coefficients calibrated for the two conditions are:  $a_n=35.66$ ,  $b_n=-0.62$ ,  $c_n=1.46$  for the natural period ( $R^2=0.97$ ), and  $a_r=0.014$ ,  $b_r=-3.67$ ,  $c_r=5.38$  for the regulated period ( $R^2=0.54$ ). The power law curves are reported in Fig. S2 in the *Supplementary Material*.

We note that, although the outflow is not directly related to the lake level in the regulated regime (see the lowest  $R^2$  of the power law), there is still a clear dependence at the annual time scale, with larger discharges associated with higher lake levels.

Having recognized that the outflow depends on the water level, we identified the equilibrium condition as the level resulting from the long-term averaged values of the input and output components and assuming no temporal variation of the lake volume, *i.e.*, solving eq. 1 for  $Q_{out}(H)$  with  $\Delta V/\Delta t=0$ . Among the 20 water balance combinations defined in the section "Over-lake evaporation and basin evotranspiration estimates", we looked for the one that provided the minimum averaged value of the residual term  $X$ . Then, we used it to define the equilibrium lake level  $H_{eq}$  (including the residual term  $X$ ). In fact, substituting  $Q_{out}$  from eq. 7 and rearranging eq. 6, we obtain the equilibrium water level as follow:

$$H_{eq,k} = \left[ \frac{P_L + P_B - ET_a - EV_L + X}{a_k} \right]^{1/c_k} + b_k \quad (\text{eq. 8})$$

In this way, we were able to assess the deviation of the lake level from its equilibrium value in response to the reduction by a given percentage of one or more water balance components.

## RESULTS

### Variability in lake evaporation and catchment evapotranspiration estimates

The comparison of various methods to estimate lake evaporation ( $EV_L$ ) and catchment evapotranspiration ( $ET_0$ ) outlines significant differences in the values to be used in the water balance, also depending on the amount of data required. To highlight such a variability, we calculated the climatological year and the statistical distribution of the  $EV_L$  and  $ET_0$  values for each day of the year, using the most "cost-effective" methods, *i.e.*, those that require the minimum number of input data: Jensen and Haise (1963, JH) for  $EV_L$  and Hargreaves and Samani (1985; HS) for  $ET_0$ . We considered the  $1\sigma$ ,  $2\sigma$ ,  $3\sigma$  as the 68<sup>th</sup>, 95<sup>th</sup> and 99.7<sup>th</sup> percentile of the distribution. Then, the statistical distributions were compared with the climatological annual cycle obtained from the other  $EV_L$  and  $ET_0$  methods. This allows for analysing the reliability of less data-requiring methods against more data-demanding methods.

By referring to Fig. 3a, in terms of  $EV_L$ , all tested methods lay within the statistical boundaries of the simplest method (JH). The only exception is represented by the Dalton (Dal) approach Fink *et al.* (2014), indicated with a green line in the plot. In fact, the inclusion of the lake surface water temperature (LSWT) required by Dal brings to a different annual cycle when compared to the other methods. This is due to the fact that over-lake air temperature (AT) and LSWT have shifted annual cycles, which is particularly notable in terms of minimum annual values (middle February against beginning of January, see

the *Supplementary Material*). Thus, the inclusion of the LSWT-AT difference within the Dal approach, known as the instability term (Fink *et al.*, 2014), allows for considering the heat storage capacity of Lake Garda, which is typical of deep lakes and shifts the minimum and maximum  $EV_L$  estimates of Dal from January to April and from July to August. The Dal method is different from the others not only because of this seasonal shift, but also in terms of annual variability of the estimated daily evaporation. The annual evaporation cycles of the Penman, 1948, (Pen), Priestley and Taylor (1972, PT) and simplified Penman Valiantzas (2006, Val) methods are contained within the  $2\sigma$  limits of JH, with minima close to  $0 \text{ mm d}^{-1}$  from December to February. Dal instead falls within the  $3\sigma$  limits only from April to August (spring-summer season), when the difference between AT and LSWT is at its minimum (constantly lower than  $5^\circ\text{C}$  (see Fig. S3b in the *Supplementary Material*). Conversely, in the rest of the year Dal falls outside the statistical boundaries of the JH method, the yearly minimum evaporation does not go

below  $2 \text{ mm d}^{-1}$  (on an annual average), as the air-water thermal gradient in winter months (see again Fig. S3b) still determines evaporation, eventually enhanced by wind and dry air conditions.

In terms of  $ET_0$  (Fig. 3c), we observe the same annual cycle among the different methods, with maximum and minimum annual values occurring in July and December, respectively. Minor differences from the HS method used as a reference are shown by its modification by Ravazzani *et al.* (2012; HSAIp) and by the FAO-56PM method, whose mean estimates are contained within the  $2\sigma$  region. The only significant distance is with the PAT (2006; PGUAP) method because of the regionally calibrated 0.7 factor included in this formulation.

The long-term estimates of  $EV_L$  and  $ET_0$  (Fig. 3 b,d) show an upward trend starting from the 1951, with a great increase starting from the 1990s in accordance with the augmented mean air and water temperature within the study area (Fig. S3c in the *Supplementary Material*). The Theil-Sen approach (Theil, 1950; Sen, 1968) indicate the slope

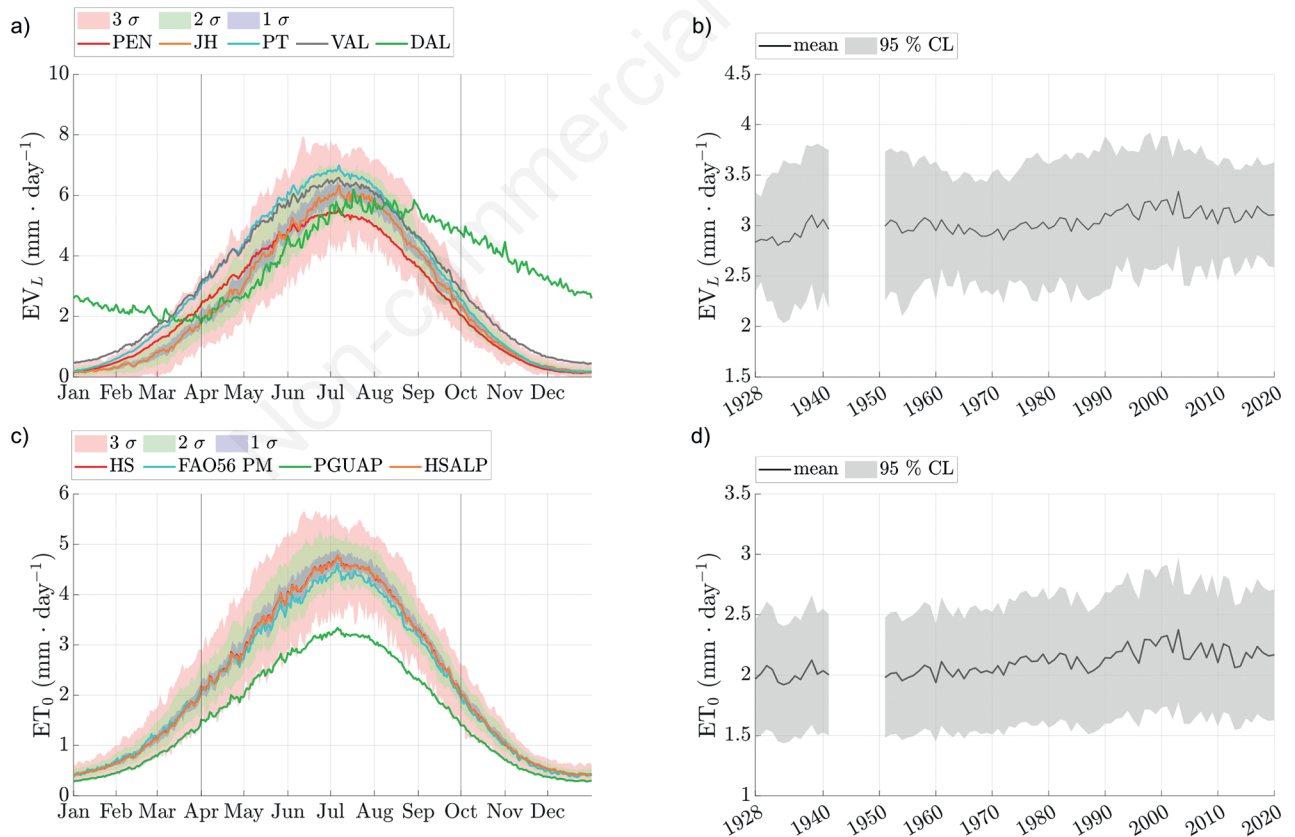


**Fig. 3.** Annual cycle and long-term trends considering the different methods adopted to estimate the over-lake evaporation (a,b) and reference evapotranspiration (c,d). The  $1\sigma$ ,  $2\sigma$ ,  $3\sigma$  in a) and c) indicate the 68<sup>th</sup>, 95<sup>th</sup> and 99.7<sup>th</sup> percentile of the statistical distribution constructed for each day of the year by referring to the less-data requiring methods of over-lake evaporation (*i.e.*, the Jansen-Haise, JH, method) and reference evapotranspiration (*i.e.*, the Hargreaves-Samani, HS, method). The vertical black lines in a) and c) split the climatological year in the warmest and coldest months. The grey shaded areas in b) and d) are referred to a 95% confidence level.

of the  $EV_L$  and  $ET_0$  trends over the period 1951-2020 as  $+0.035 \text{ mm d}^{-1}/\text{decade}$  and  $+0.033 \text{ mm d}^{-1}/\text{decade}$ , respectively, with a major increase during the 1990-2000 decade ( $+0.16 \text{ mm d}^{-1}/\text{decade}$  and  $+0.12 \text{ mm d}^{-1}/\text{decade}$ ). Such trends are evaluated with a 95% confidence level (grey shaded area), with similar intervals (2s limits) for both  $EV_L$  and  $ET_0$  ( $\pm 0.6 \text{ mm d}^{-1}$  and  $\pm 0.5 \text{ mm d}^{-1}$ , respectively, on average). We note, however, that the confidence intervals are largely affected by the inclusion of the Dal method for  $EV_L$  and PGUAP method for  $ET_0$ , without which they would shrink to  $\pm 0.1 \text{ mm d}^{-1}$ .

### Long-term variation of water balance components

The water balance equation (eq. 1), was applied on an annual basis (hydrological year from 1<sup>st</sup> October to 30<sup>th</sup> September) for the 20 combinations of over-lake evaporation and catchment evapotranspiration methods introduced in the section “Over-lake evaporation and basin evotranspiration estimates”. The combination that minimized the residual term  $X$  over the entire time period was provided by the Pen evaporation model and PGUAP evapotranspiration approximation. As reported in Fig. 4a, the PGUAP-based  $ET_0$  allowed for the lowest median value

of  $X$ , while presenting similar variability in terms of 25<sup>th</sup> and 75<sup>th</sup> and percentiles. The  $EV_L$  estimate was less influential, with the Penman and JH methods providing the lowest median value of  $X$  (red lines of PGUAP-Pen and PGUAP-JH in Fig. 4a), estimated as  $2.99 \text{ m}^3\text{s}^{-1}$  and  $3.03 \text{ m}^3\text{s}^{-1}$ , respectively.

The magnitude and long-term tendency of the water balance components (WBCs) included in eq. 6 are shown in Fig. 4b, together with the residual term  $X$  of the optimal combination. In Tab. 4 are summarised the average values of the single WBCs estimated in the two analyzed periods (1928-1941 and 1951-2020) together with their range of variation. The statistics of the term  $X$ , obtained as the average from the analysis of all the combinations, are reported in the table together with the values evaluated for the optimal combination ( $X_{opt}$ ). We noted that a significant statistical comparison between the pre-regulation and post-regulation periods is limited by the lack of a sufficient number of data for the former time period. Despite this data limitation, mostly related to a minor number of gauging stations in the first decades of the XX century, we consider such comparison as a useful information for comparing the results of the two periods.

**Tab. 4.** Statistics of the Lake Garda water balance components (WBCs).

WBC	1928-1941				1951-2020			
	Min/Max ( $\text{m}^3\text{s}^{-1}$ )	Mean ( $\text{m}^3\text{s}^{-1}$ )	$\sigma$ ( $\text{m}^3\text{s}^{-1}$ )	CV (-)	Min/Max ( $\text{m}^3\text{s}^{-1}$ )	Mean ( $\text{m}^3\text{s}^{-1}$ )	$\sigma$ ( $\text{m}^3\text{s}^{-1}$ )	CV (-)
$P_B$	56.4/92.1	70.7	11.7	0.17	46.1/111.2	68.6	12.4	0.18
$P_L$	9.6/15.0	11.8	1.9	0.16	8.4/19.7	12.3	2.2	0.18
	-8.2/6.7	-0.2	4.8	-	-14.3/9.1	0.03	3.9	-
	9.8/10.6	10.2	0.2	0.02	10.1/11.9	10.8	0.3	0.03
	9.5/10.9	10.2	0.4	0.04	-13.3/-9.9	11.4	0.7	0.06
	12.4/13.4	12.8	0.3	0.03	12.7/14.9	13.6	0.4	0.03
	12.3/14.0	13.1	0.50	0.04	12.9/15.4	14.0	0.52	0.04
	14.0/17.0	16.1	0.89	0.06	14.4/17.2	15.9	0.71	0.04
Mean $EV_L$	9.5/17.0	12.5	0.47	0.04	10.0/17.2	13.1	0.54	0.04
	23.5/26.9	25.1	0.92	0.04	26.2/31.2	28.0	0.93	0.03
	16.4/18.8	17.6	0.64	0.04	18.3/21.8	19.6	0.65	0.03
	22.4/25.7	24.1	0.88	0.04	25.5/30.4	27.1	0.95	0.04
	24.4/28.3	26.3	1.04	0.04	27.2/32.6	29.1	0.99	0.03
Mean $ET_a$	16.4/28.3	23.3	0.87	0.04	18.3/32.6	25.9	0.88	0.03
$Q_{out}$	49.6/91.6	63.3	11.4	0.18	26.6/122.0	52.5	15.5	0.30
$X$	12.4/47.6	19.0	16.0	-	-23.0/61.5	9.2	15.2	-
$X_{opt}$	-2.3/32.0	10.5	16.0	-	-23.0/48.4	0.9	14.8	-

CV, /mean is the coefficient of variation;  $P_B$ , catchment precipitation;  $P_L$ , over-lake precipitation;  $EV^{Pen}$ , over-lake Penman (1948) evaporation;  $EV^{JH}$ , over-lake Jensen and Haise (1963) evaporation;  $EV^{PT}$ , over-lake Priestley and Taylor (1972) evaporation;  $EV^{Val}$ , over-lake Valiantzas (2006) evaporation;  $EV^{Dal}$ , over-lake Dalton (Fink *et al.*, 2014) evaporation; mean  $EV_L$ , over-lake evaporation as the mean between the different models considered; , catchment Hargreaves and Samani (1985) evapotranspiration; , catchment Provincia Autonoma di Trento (2006) evapotranspiration; , modified HS catchment evapotranspiration (Ravazzani *et al.*, 2012); , FAO-56 Penman-Monteith catchment evapotranspiration (Allen *et al.*, 1998);  $X$ , residual term as the average of all the 20 possible WB combinations;  $X_{opt}$ , residual term considering the optimal combination; mean  $ET_a$ , catchment evapotranspiration as the mean between the different models considered; Min/Max, minimum and maximum annual values; mean, mean annual value;  $\sigma$ , standard deviation.

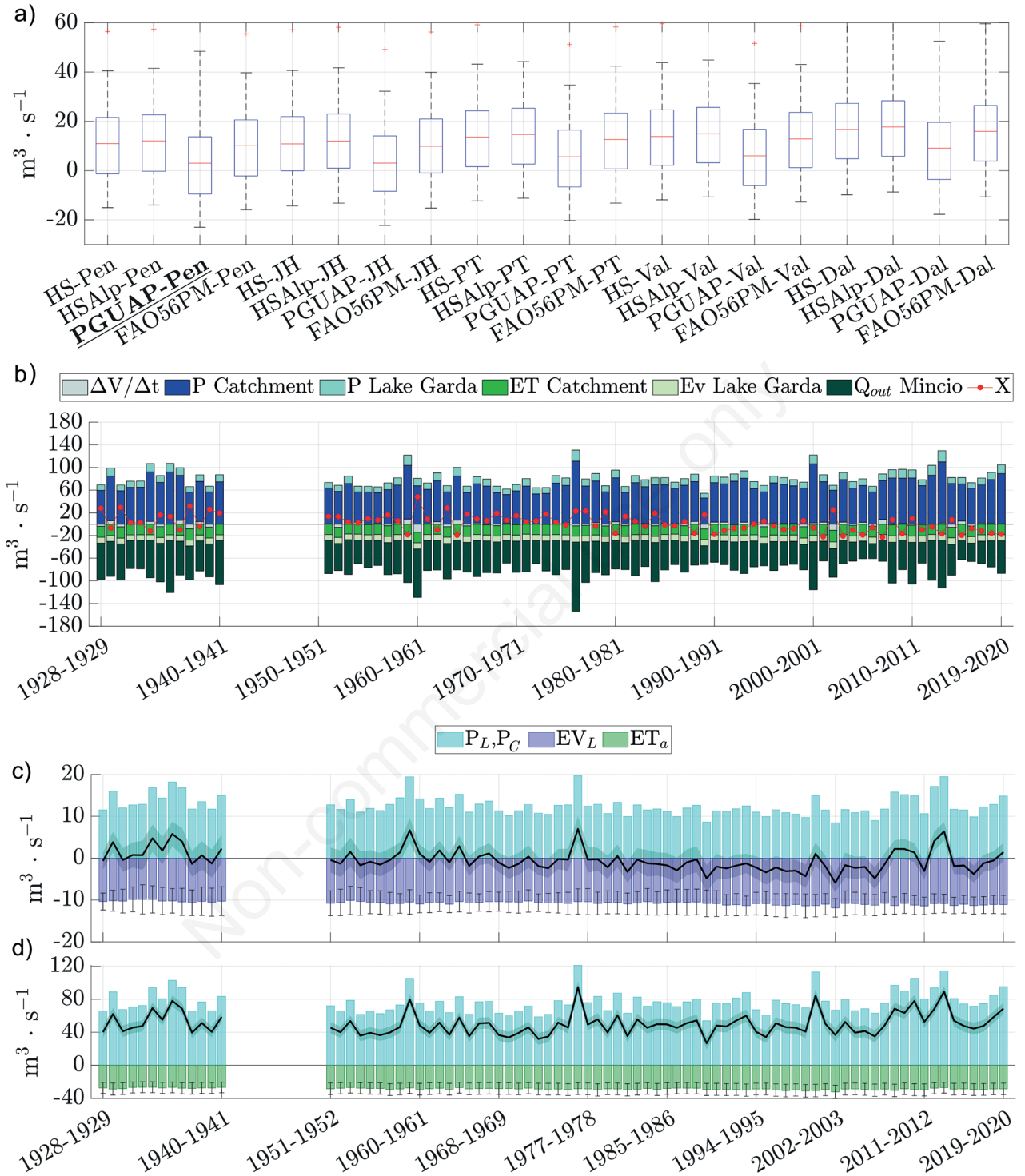


**Fig. 4.** Box-plot of the residual term  $X$  obtained from the different water balance combinations of  $EV$  and  $ET_a$  (in the x axis according to Tab. 2) over the entire period of analysis; the combination that provides the minimum average value of  $X$  is indicated with a bold and underlined font. b) Water balance of Lake Garda in the periods 1928-1941 and 1951-2020, separated into its main components averaged over a hydrological year (October-September). The  $EV$ ,  $ET_a$  and  $X$  components refer to the method that provides the minimum  $X$  absolute value. c) Annual difference (black solid line) between over-lake precipitation and evaporation (coloured bars), and d) catchment precipitation and actual evapotranspiration  $ET_a$ . Gray shaded areas and vertical lines are computed considering a 95% confidence level referred to the over-lake evaporation and catchment evapotranspiration variability. c-d) Annual difference (black solid line) between over-lake precipitation  $P_L$  and evaporation  $EV_L$  (coloured bars), and catchment precipitation  $P_C$  and actual evapotranspiration  $ET_a$ .

The precipitation over the catchment  $P_C$  is the most important contribution to the lake overall water budget. The mean value of this term ( $70.7 \text{ m}^3\text{s}^{-1}$ ) is almost six times greater than the over-lake precipitation  $P_L$  ( $11.8 \text{ m}^3\text{s}^{-1}$ ). On average, both  $P_C$  and  $P_L$  mean values are lower in the second period of analysis (1951-2020) than in the first (1928-1941) of  $-2.1 \text{ m}^3\text{s}^{-1}$  and  $-0.5 \text{ m}^3\text{s}^{-1}$ , respectively.

In terms of catchment actual evapotranspiration ( $ET_a$ ), we observe an increment of  $2.6 \text{ m}^3\text{s}^{-1}$  on average between the two periods considered, whereas the over-lake evaporation  $EV_L$  increased of  $1.6 \text{ m}^3\text{s}^{-1}$  (in both cases considering the average value among the different methods considered here). In addition, the mean values reported in Tab. 4 highlight that  $ET_a$  represents the 33% (1928-1941) and 37% (1951-2020) of  $P_B$ , in line with the typical value of 30% as reported by McMahon *et al.* (2013). The lake volume variation ( $\Delta V/\Delta t$ ), which reflects the lake's water level annual oscillations, shows higher maximum and minimum values during the period 1951-2020 but a smaller standard deviation  $\sigma$  ( $3.9 \text{ m}^3\text{s}^{-1}$  against  $4.8 \text{ m}^3\text{s}^{-1}$ ). In terms of coefficient of variation (CV), precipitation and lake outflow present values one order of magnitude higher than those of the  $EV_L$  and  $ET_a$ . The CV values of precipitation and lake outflow are of similar entity for the pre-regulation period (0.16 against 0.18), whereas the CV of the lake outflow almost doubles after lake regulation (0.30).

The residual term  $X$  is characterized, considering its average on the 20 combinations, by a positive mean value, possibly indicating the lack of some input contribution or even the overestimation of the output components. In particular, the general deficiencies in the  $X$  term might be related to unaccounted deep aquifer dynamics, including potential input contributions from sublacustrine sources (Zorzin and Tottola, 2020). However, a more careful analysis of the temporal variation (Tab. 4) shows a relevant reduction in the post-regulation period: from  $19.0 \text{ m}^3\text{s}^{-1}$  in 1928-1941 to  $9.2 \text{ m}^3\text{s}^{-1}$  in 1951-2020.

Moreover, the averaged  $X$  values of Tab. 4 reveal higher mean values when compared to the results obtained from the optimal combination  $X_{opt}$  (adopting the Pen and PGUAP methods), *i.e.*,  $10.5 \text{ m}^3\text{s}^{-1}$  (1928-1941) and  $0.9 \text{ m}^3\text{s}^{-1}$  (1951-2020), reflected also by a reduction of  $-15.6 \text{ m}^3\text{s}^{-1}$  (1928-1941) and  $-13.1 \text{ m}^3\text{s}^{-1}$  (1951-2020) in the maximum values recorded.

The variability of  $X$  decreases in the second period as well ( $16.0 \text{ m}^3\text{s}^{-1}$  against  $15.2 \text{ m}^3\text{s}^{-1}$ ), but higher extremes are registered, as indicated by the maximum and minimum values. As shown in Fig. 4b, the residual term  $X_{opt}$  of the optimal combination reveals a downward tendency in the second period of analysis, with its mean value passing from positive (1951-1989 average:  $+7.4 \text{ m}^3\text{s}^{-1}$ , *i.e.*, under/overestimation of the total water inputs/outputs) to almost neutral (1990-2002 average:  $-2.7 \text{ m}^3\text{s}^{-1}$ ) to negative

(2003-2020 average:  $-10.2 \text{ m}^3\text{s}^{-1}$ , *i.e.*, under/overestimation of the total water outputs/inputs).

Such a tendency calls into question the influence of the long-term trends of the different WBCs on the unaccounted contributions. Besides the increasing trend of  $EV_L$  and  $ET_a$ , triggered by the augmented air and water temperature starting from the 1990s (see Fig. S3c in the *Supplementary Material*), a major influence might be related to the lake outflows and the catchment precipitation. In particular, while outflows show a significant downward trend after the lake regulation (with a mean value of  $10.8 \text{ m}^3\text{s}^{-1}$  lower than the pre-regulation period), an increasing trend is observed for the difference between precipitation and evapotranspiration starting from the 2000s (Fig. 4b).

In addition, we note occasionally high values of  $X$  concurrent with significant variations of the lake's volume ( $\Delta V/\Delta t$ ), but with opposite sign (*e.g.*, 1929, 1936 and 1937, 1960 and 2002). This occurrence provides some insights on the response time of Lake Garda's water levels to relevant floods, and the potential influence of the outflow regulation through the Salionze Dam management. For instance, the flood event of 17-21 September 1960 occurred at the end of the hydrological year (30<sup>th</sup> September 1960). The Sarca River peak flood was registered as  $394 \text{ m}^3\text{s}^{-1}$  and determined an increase of the lake's water level up to 2.12 m above the reference level (annual  $\Delta V/\Delta t = +9 \text{ m}^3\text{s}^{-1}$ ). Such major variation of the storage was restored to normal conditions just during the subsequent hydrological year (1960-1961) by discharging  $85 \text{ m}^3\text{s}^{-1}$  at the outlet, producing a consistent lowering of the lake level (annual  $\Delta V/\Delta t = -14 \text{ m}^3\text{s}^{-1}$ ). Thus, the large variation of the storage resulted from a temporary event during the transition from one hydrological year to the following one. In fact, all red crosses in the boxplots of Fig. 4a indicate the value of  $X$  found for the flood event of 1960: the statistics confirm that such value is an outlier for the 20 combinations of the water balance. In Tab. 4,  $X_{max}$  value for the period 1951-2020 ( $61.5 \text{ m}^3/\text{s}$ ) refers to this relevant flood event.

### Splitting the water balance between the lake and its catchment

In addition to the overall water balance of Lake Garda, in Fig. 4 c-d, we examine the evaporation  $EV_L$  from the lake surface and the actual evapotranspiration  $ET_a$  from the overall contributing catchment (Sarca, Ledro and minor catchments) separately, and compare them with their input counterparts, *i.e.*, over-lake and catchment precipitation ( $P_L$  and  $P_B$ ). The net over-lake balance is represented by the difference  $P_L - EV_L$ . Instead, we consider as water yield of the catchment the difference  $P_B - ET_a$  (Budyko, 1974), which in turn represents our estimate of the total inflows as detailed in the section "Estimation of inflows". The two sub-balances were computed including all the different  $EV_L$

and  $ET_0$  methods, defining the related mean value and 95% confidence intervals.

The mean annual values of over-lake balance and water yield range from  $7.9 \text{ m}^3\text{s}^{-1}$  to  $-5.4 \text{ m}^3\text{s}^{-1}$  ( $P_L - EV_L$ ) and from  $27.5$  to  $95.6 \text{ m}^3\text{s}^{-1}$  ( $P_B - ET_a$ ). The variation of the sub-balances is mostly driven by the higher precipitation variability if compared to the one of  $EV_L$  and  $ET_a$ , as the maximum and minimum annual values of water yield and over-lake balance are generally in accordance with the highest and lowest annual precipitation estimates. The absolute maximum was recorded in 1960 ( $P_L=19.7 \text{ m}^3\text{s}^{-1}$ ,  $P_B=121.2 \text{ m}^3\text{s}^{-1}$ ), while the absolute minimum in 1989 ( $P_L=8.6 \text{ m}^3\text{s}^{-1}$ ,  $P_B=53.9 \text{ m}^3\text{s}^{-1}$ ).

In terms of over-lake balance, we observe a decreasing trend of  $P_L - EV_L$  starting from the second period of analysis (1951-2020), with slope of  $-0.28 \text{ m}^3\text{s}^{-1}/\text{decade}$  according to the Theil-Sen approach, and constantly negative values for the decade 1989-1999 ( $-2.8 \text{ m}^3\text{s}^{-1}$  on average). We note that the over-lake balance trend would become more marked ( $-0.30 \text{ m}^3\text{s}^{-1}/\text{decade}$ ) the Dalton method were not included in the options for the computation of  $EV$ , as it determines an increase of  $0.7 \text{ m}^3\text{s}^{-1}$  of the net over-lake balance (averaged over the entire period of analysis). A negative over-lake balance was already estimated by Berbenni *et al.* (1992) ( $-2.3 \text{ m}^3\text{s}^{-1}$  on average).

Different from the over-lake balance ( $P_L - EV_L$ ), the catchment water yield ( $P_B - ET_a$ ), is characterized by a constantly positive value, always larger than  $40 \text{ m}^3\text{s}^{-1}$ . Such difference increases in the last decade, passing from  $56 \text{ m}^3\text{s}^{-1}$  (1951-2009) to  $62 \text{ m}^3\text{s}^{-1}$  (2010-2020).

### Sensitivity analysis

We finally performed a sensitivity analysis to evaluate which water balance component mainly controls the equilibrium lake water level ( $H_{eq}$ ) and outflow ( $Q_{out,eq}$ ). The analysis also provides a measure to understand how the uncertainties related to the estimation of each water balance component may alter the lake level and outflow. Fig. 5 shows how the perturbation of the Lake Garda water level and outflow are primarily driven by catchment precipitation ( $P_C$ ) followed by catchment evapotranspiration ( $ET_a$ ). The plot reports also the influence of total inflow from the surrounding catchments (Sarca, Ledro and minor tributaries), which is assumed to be directly related to catchment precipitation and actual evapotranspiration ( $Q_{in}=P_C-ET_a$ ; eq. 5). This information is redundant but useful to illustrate the dynamics in comparison with the trend assumed by the catchment precipitation. Finally, the over-lake evaporation and precipitation ( $EV_L$  and  $P_L$ ) play a secondary role, with opposite effects but similar magnitude, on both  $H_{eq}$  and  $Q_{out,eq}$ .

The influence of precipitation ( $P_C$  and  $P_L$ , and

consequently of the total catchment inflow,  $Q_{in}$ ) on  $H_{eq}$  largely diminishes in the post-regulation period (1951-2020; solid lines in Fig. 5a). This behaviour highlights the mitigation effect of the dam operational rules on the Lake Garda water level variation. Conversely, evaporation and evapotranspiration maintain a similar effect on  $H_{eq}$  before and after the lake regulation. Similarly, the equilibrium value of the Lake Garda outflow (Fig. 5b), which reflects

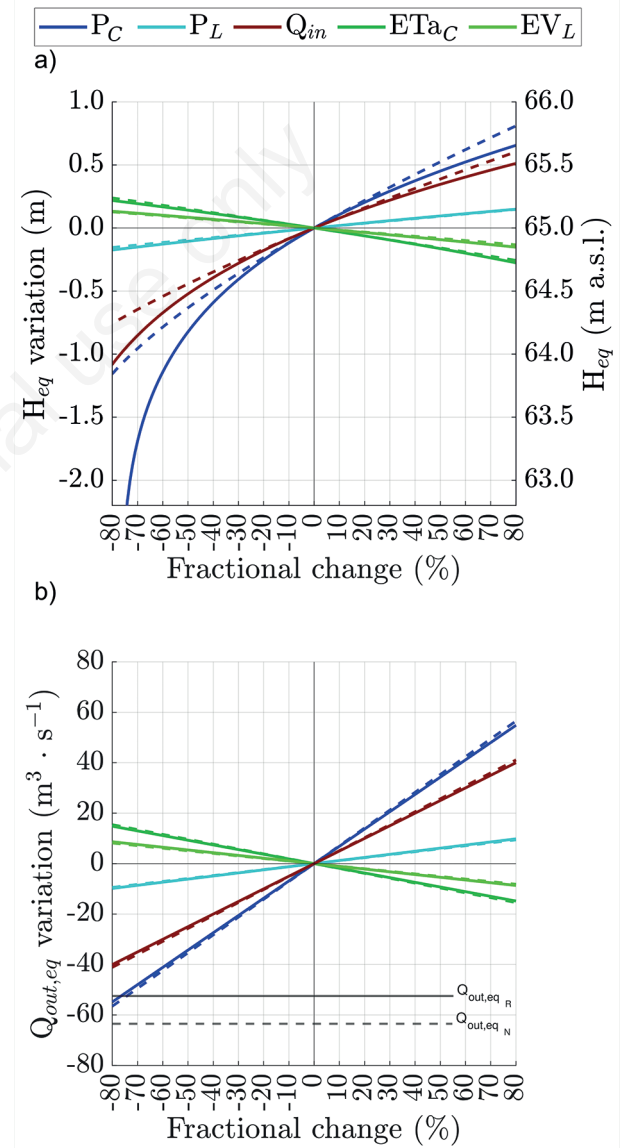


**Fig. 5.** Sensitivity analysis on the Lake Garda. a) Equilibrium water level  $H_{eq}$ . b) Outflow  $Q_{out,eq}$  performed following eq. 8. The variation of  $H_{eq}$  (or  $Q_{out,eq}$ ) is obtained by altering one of the water balance components by a specific percentage (hereby named fractional change). The origin point of the plot (no variation) represents the equilibrium value of lake level (or outflow). The dashed lines refer to the pre-regulation period (1928-1941), while the solid lines indicate the post-regulation period (1951-2020).

the Mincio River discharge, is mostly sensitive to variations of  $P_C$ .

As for the entity of the variations of  $H_{eq}$  and  $Q_{out,eq}$ , we see that an increment of, *e.g.*, 25% of  $ET_a$  would decrease the lake level of some 0.07 m, corresponding to 25.7 Mm<sup>3</sup> of lake volume. Under the current regulated conditions, an increase of 25% of the  $P_C$  would determine an increment of 0.12 m of  $H_{eq}$ , while it would have been of 0.27 m over the pre-regulation regime. The great influence of  $P_C$  on the lake variation is also underlining by the asymptotic behaviour assumed by  $H_{eq}$  in the regulated period when reducing the contribution of  $P_C$  by more than 77%. A fractional change of 25% in  $EV_L$  would decrease the lake level of 0.04 m (*i.e.*, of 14.7. Mm<sup>3</sup> of lake volume) both in the pre- and post-regulation periods, while  $P_L$  would increase the lake level of 0.05 m and 0.03 m, respectively. In light of the long-term trends presented in Fig. 4 c,d), considering the  $H_{eq}$  for the periods 1951-1989 and 1990-2020 separately, the modification of  $EV_L$  (with a 25% of fractional change) reveal a decreasing impact on the lake level variation from 0.047 m to 0.026 m, respectively. In terms of lake outflows, diminishing the  $P_C$  by 10% would reduce  $Q_{out,eq}$  of 7 m<sup>3</sup>s<sup>-1</sup>. We note that this value is close to the total environmental flow discharge established for the Mincio River by the current management policy (6 m<sup>3</sup>s<sup>-1</sup>).

## DISCUSSION

The computation of the multidecadal water balance of Lake Garda outlined the role of the different terms contributing to the overall water budget of the Sarca-Garda system. Our analysis considered the role played by the number and kind of hydro-meteorological data adopted as inputs. In this way, our study provides an overview of the long-term evolution of one of the major water resources of the Italian Alpine context, following some other relevant works carried out within this area, especially the multi-century (1845-2016) meteo-hydrological analysis for Lake Como carried out by Ranzi *et al.* (2021). In particular, the approach adopted in Ranzi *et al.* (2021) to explore the rainfall and runoff variability (*i.e.*, North Atlantic Oscillation (NAO), Atlantic Multidecadal Oscillation and Western Mediterranean Oscillation indexes and sunspot activity) could also be applied to the Lake Garda catchment to discuss regional patterns within the Alpine area. Thanks to a multi-method approach, we also explored the relative weight of the over-lake evaporation and catchment evapotranspiration terms based on the chosen method for their estimation. By including a residual term  $X$  in the water balance equation, we discussed the possible influence of additional, unresolved components and their long-term trend. Here, we discuss our results on the residual term  $X$  and the potential contributions to its magnitude. We recall, however, that the proper estimate of this term highly

depends on the accuracy of the other components of the water balance, *e.g.*, surface inflows or precipitation (Kampf *et al.*, 2020). In addition, we state that the optimal WBC found, *i.e.*, the one obtained from the Pen evaporation and PGUAP evapotranspiration, might be different by increasing the number of records adopted within the analysis, especially in terms of the Sarca River discharge for calibrating the inflows.

In several cases, the residual term is related to the groundwater fluxes (Hood *et al.*, 2006; Li *et al.*, 2007; Zhou *et al.*, 2013). A similar supposition was made also for Lake Garda (Berbenni *et al.*, 1992; Longinelli *et al.*, 2008), but a proper quantification of the groundwater fluxes and the related drainage timing is still lacking. In particular, Berbenni *et al.* (1992) state that the residual unresolved term was mainly attributed to the neglected groundwater fluxes upstream the Lake Garda catchment as well as to the fluxes through the geological formations in the Mount Baldo area. The total estimated average value of the residual is 7 m<sup>3</sup>/s. Based on the isotopic values and the available hydrological data, Longinelli *et al.* (2008) concluded that large amounts of groundwater flow into the lake and can explain the input-output imbalance found. In comparison, here we estimated the groundwater fluxes due to Mount Baldo catchment in the range 2.7-8.5 m<sup>3</sup>/s, with an average value of 4.7 m<sup>3</sup>/s, while the groundwater component of the Sarca Catchment is indirectly estimated with the choice of hydrological year for the balance evaluation.

The time scale of the analysis is crucial. In our analysis, we argue that the net precipitation (*i.e.*,  $P_B - ET_a$ ) on the whole lake's drainage catchment can be considered as a plausible proxy of the total water contributions to the lake water balance on an annual time scale, including groundwater fluxes. In fact, a large part of the water that penetrates and reaches the subsurface reservoir is expected to flow into the streams and contribute to the lake's water balance on this time scale. Nevertheless, results might be affected by deep aquifer dynamics and possible delays in the drainage. In this regard, the lack of reliable data on the Sarca River (*i.e.*, the major lake tributary) to quantify its inflow discharge is of special concern, especially in light of the growing role of hydroelectricity production within its catchment over the last century. Likewise, snow melt and its long-term variation within the lake's catchment (and particularly again within the Sarca River catchment) might have changed the annual contribution of surface water flows throughout the years. In fact, in order to account for the water stored as snow or ice in the catchment, we set the start of our hydrological year in October, the latest time to consider the melted water reaching the lake before the accumulation in the cold season for the new year.

In addition to such factors, here we discuss the role of Mount Baldo, whose role has been questioned in the past.

Besides the contribution provided by the west side of the mount, whose rainfall is naturally conveyed into the lake, an additional contribution might be given by the east side, as its dip slope structure and calcareous morphology is likely an additional input contribution to Lake Garda, both in terms of surface and subsurface fluxes (Zorzin and Tottola, 2020). Hence, we included the net precipitation ( $P_B - ET_a$ , which we assume is transformed into  $Q_{in}$ ) over the Mount Baldo catchment in an alternative water balance using the same procedure detailed in eq. 4 ( $Q$  term) and in eq. 1 ( $Q_i$  term). Similarly to what was obtained for the water balance analysis without considering the Mount Baldo contribution, the analysis of all the 20 possible combinations that minimize  $X$  was provided by selecting the Pen  $EV_L$  and PGUAP  $ET_0$  methods. Thus, starting from such water balance combination that minimizes the value of  $X$  (Fig. 4a), we compare the estimates of  $X$  from this new configuration with those obtained without considering the contribution of Mount Baldo catchment. Results are reported in Fig. S1 (*Supplementary Material*) for discussion. The Mount Baldo drainage catchment contributes with an average input of  $4.2 \text{ m}^3\text{s}^{-1}$  (Fig. S1a, *Supplementary Material*). Thus, its inclusion in the water balance of Lake Garda reduces (in absolute terms) the value of  $X$  until the 1990s, when  $X$  starts to assume negative values (Fig. S1b, *Supplementary Material*). However, by computing the difference between the mean absolute value of  $X$  (averaged on all the 20 possible combinations of the water balance) with and without the Mount Baldo area, we obtain a reduction of  $4.6 \text{ m}^3\text{s}^{-1}$  and  $2.0 \text{ m}^3\text{s}^{-1}$  for the 1928-1941 and 1951-2020 periods, respectively. A general reduction of the  $X$  terms was also noted by comparing the average values calculated for all the 20 possible combinations with and without including Mount Baldo as was carried out in Tab. 4. In particular, the statistics of  $X$  considering the Mount Baldo catchment indicate significant lower values for the maximum ( $14.8 \text{ m}^3\text{s}^{-1}$  against  $47.6 \text{ m}^3\text{s}^{-1}$  and  $23.6 \text{ m}^3\text{s}^{-1}$  against  $61.5 \text{ m}^3\text{s}^{-1}$ ), mean ( $-7.8 \text{ m}^3\text{s}^{-1}$  against  $19.0 \text{ m}^3\text{s}^{-1}$  and  $-3.8 \text{ m}^3\text{s}^{-1}$  against  $9.2 \text{ m}^3\text{s}^{-1}$ ) and s ( $8.2 \text{ m}^3\text{s}^{-1}$  against  $16.0 \text{ m}^3\text{s}^{-1}$  and  $9.6 \text{ m}^3\text{s}^{-1}$  against  $15.2 \text{ m}^3\text{s}^{-1}$ ).

These results indicate that the inclusion of the Mount Baldo area within the Lake Garda water balance computation contributes to reducing the magnitude of the  $X$  term. In addition, we noticed that this effect is reduced starting from 1990. Another possible source of uncertainty is related to the land use/land cover and its evolution throughout the years, as its value influences the potential evapotranspiration ( $ET_p$ ) of the drainage catchments of Lake Garda. By following the land use evolution within the catchment over the last century, we observed significant changes occurring from 1970 onward (Figure a in the Appendix). In particular, we note a consistent increment of

urban and forest areas, and a concurrent decrease of the pasture and cropland areas. This change causes an overall reduction of the mean annual crop coefficient  $K_c$  (Fig. S5b in the *Supplementary Material*) (Ranzi *et al.*, 2017; Balistrocchi *et al.*, 2021). In order to test how such a long-term  $K_c$  variation affects the final  $ET_p$  estimates, we applied the mean  $K_c$  characterizing the first period of analysis (1928-1941) to the  $ET_0$  of the second period (1951-2020) for all the four methods considered in the analysis. A little difference (average of all methods  $<0.1 \text{ mmday}^{-1}$ , *i.e.*,  $<2.2 \text{ m}^3\text{s}^{-1} \text{ day}^{-1}$ ) was found with respect to the  $ET_p$  estimated with the correct  $K_c$ s. In addition, we also investigated whether the number of land use categories is relevant for the  $ET_a$  estimates in our study area. Hence, we estimated the  $K_c$  coefficient based on the Corine Land Cover (CLC) dataset (44-classes land cover maps with spatial resolution of  $100 \text{ m} \times 100 \text{ m}$  since 1990), and eventually compared the results with  $ET_a$  estimated from the HILDA+ dataset (7-classes land cover maps with spatial resolution of  $1 \text{ km} \times 1 \text{ km}$  over the period 1899-2019; Winkler *et al.*, 2020). As shown in Fig. S5c in the *Supplementary Material*, the CLC inventory determined a marginally lower average  $K_c$  value and a final  $ET_a$  estimate up to  $0.5 \text{ mmday}^{-1}$  lower than the values obtained from the HILDA+ dataset. The marginal variation of the catchment evapotranspiration obtained with different land use datasets confirm the lower influence of this component in altering the lake equilibrium, as we found in our sensitivity analysis in terms of lake level and outflow variations.

To further underpin the results obtained in our study, alternative approaches could be implemented. Examples are given by stable isotopes analyses (Gibson and Edwards, 2002; Tian *et al.*, 2008; Longinelli *et al.*, 2008; Turner *et al.*, 2010; Cui *et al.*, 2018), which require continuous sampling campaigns, or remote sensing studies (Swenson and Wahr, 2009; Jiang *et al.*, 2017; Mohebzadeh and Fallah, 2019). Furthermore, the uncertainties related to the lake water balance computation have been recently investigated through different statistical techniques in several studies to improve the estimates of the different components. For instance, a Bayesian framework was proposed for the Laurentian Great Lakes catchment (Gronewold *et al.*, 2020; Do *et al.*, 2020). Such alternative approaches could help quantifying the entity of the inaccuracies and provide valuable information on the reliability of the hydro-meteorological data recorded by the existing gauging stations (Kampf *et al.*, 2020). In this regard, designing strategic monitoring plans and ensuring a comprehensive network of hydro-meteorological gauging stations can improve the computation accuracy of the water balance, though uncertainties cannot be completely removed (Kampf *et al.*, 2020).

In light of the fragmented administration and the large number of water interests characterizing the Lake Garda

catchment, we outline the importance of ensuring a consistent hydro-meteorological database, with data recorded through a unique and concerted standard. In this regard, the large database of daily hydro-meteorological data constructed within this study represents a unique source of information to support integrated water resources management investigations in the Lake Garda system, which are still limited (Salmaso and Mosello, 2010). Additionally, such database can boost further studies on different ecological and water quality aspects, given their interdependence with hydro-meteorological factors. The creation of a freely accessible geo-portal would promote lake monitoring projects (Baracchini *et al.*, 2020), as well as a participatory approach that can sustain water resources management in the area (Voinov *et al.*, 2016; Amadori *et al.*, 2020). In this regard an open access comprehensive database of the collected hydro-meteorological data will be provided.

---

## CONCLUSIONS

The main results of the paper can be summarized as follows:

- i) a consistent hydrometeorological database for the Lake Garda catchment has been constructed starting from different sources. This dataset will be systemized in a comprehensive online geoportal for public access, supporting future investigations in the area;
- ii) the multi-method approach adopted within the computation of the water balance provided an indication of the relative weight of the over-lake evaporation and catchment evapotranspiration terms based on the chosen method for their estimation, highlighting their suitability for the study area
- iii) site-specific calibrated methods, such as the PGUAP formula, provide more reliable results than not site-specific methods within the water balance computation
- iv) the value of the unresolved term  $X$  provided an indication of the unaccounted contributions, including the deep groundwater fluxes, a finding that has already been shown in previous works (Berbenni *et al.*, 1992; Longinelli *et al.*, 2008).

We analysed the multidecadal water balance of Lake Garda, monitoring the long-term evolution of its main components and detecting their relative influence on determining the lake level variation. In order to reduce the errors about the quantification of the water storage in snow and ice reservoirs at high elevation, we aggregated the lake's WBCs on an annual basis, assuming the hydrological year from October to September (end of the melting season). The annual aggregation also allowed us to reduce the uncertainties in the estimate of the groundwater contribution with respect to the surface streams.

Being aware of the many alternative formulations to

compute some terms of the water balance (in particular, over-lake evaporation and catchment evapotranspiration), we tested different combinations of the most used empirical relations. Through this multi-method analysis, we recognized how the amount of available data influences the estimates, for instance producing quite different annual cycles of evaporation when using the Dalton formula with respect to the Penman approach. Testing the different combinations, we found the one that minimizes the entity of the residual term  $X$ , which includes both the errors in the estimates and the unaccounted contributions (*e.g.*, the groundwater fluxes or the temporary storage across two consecutive years). Then, it was possible to analyse the variation in time of  $X$ , calling in questions the evolution of possible unaccounted contributions, as well as the uncertainty related to the WBC estimates depending on the quality of the data. As expected, the estimate of the WBCs indicated a major influence of precipitation in controlling the water availability within the catchment; such a result was confirmed by a sensitivity analysis that we performed by looking at the relative contribution of the different WBCs on the water level fluctuations.

The long-term analysis allowed us to distinguish some trends in the input and output components of the water balance. Two major changes can be highlighted. First, after the impoundment of Lake Garda in 1951, the outflow has been artificially regulated and the relationship between the water level and the outflow discharge has changed. This change modified the sensitivity to the different WBCs, as well. Second, some effects of the climatic alteration can be seen, especially in the last three decades. Among them, a change in the sign of the residual component  $X$  could be detected, suggesting a transition from a general underestimation of the input terms (or overestimation of the output) to an overestimation in the last two decades. The reasons for such a behaviour are still unknown.

Knowing the effect of the WBCs on the availability of the water resource is of primary importance for the management of Lake Garda, where different water uses are present and are all characterized by high economic relevance. The potential conflict, together with the lack of coordination produced by the trans-regional administration, makes any choice for the water management critical in this area. In this respect, our contribution represents the first necessary step towards the definition of a common background for the definition of policies the local stakeholders can agree on.

---

## ACKNOWLEDGMENTS

The contributions of Nicola Malesardi and Valentina Trenti to the preliminary data collection and setup of the water budget of Lake Garda are gratefully acknowledged. Authors thank the support and data provided by the

Interregional Agency for the Po River (AIPo). Data and information made available through the freely accessible online portals by the Regional Agencies of Lombardia (ARPAL, [www.arpalombardia.it](http://www.arpalombardia.it)), Veneto (ARPAV, [www.arpa.veneto.it](http://www.arpa.veneto.it)), the Autonomous Provinces of Trento (PAT) [www.meteotrentino.it](http://www.meteotrentino.it) and Bolzano (PAB, [www.meteo.provincia.bz.it](http://www.meteo.provincia.bz.it)) and the Comunità del Garda ([www.comunitadelgarda.it](http://www.comunitadelgarda.it)) are also thankfully acknowledged. The authors wish to thank ARPAV for providing additional historical daily meteorological data of the Veneto Region. The authors thank the Research Office of Mu.Se. of Trento (in particular Christian Casarotto and Massimo Bernardi) that provided detailed DTMs of the glaciers in the Trentino-Alto-Adige Region. This work has been supported by the Italian Ministry of Education, University and Research (MIUR) in the frame of the “Departments of Excellence” Grant L. 232/2016. The publication was created with the co-financing of the European Union - FSE-REACT-EU, PON Research and Innovation 2014-2020 DM1062/2021.

## REFERENCES

- Adrian R, O'Reilly CM, Zagarese H, Baines SB, Hessen DO, Keller W, et al., 2009. Lakes as sentinels of climate change. *Limnol Oceanogr* 54:2283–2297.
- Allen RG, Pereira LS, Raes D, Smith M, 1998. Crop evapotranspiration-guidelines for computing crop water requirements - FAO irrigation and drainage paper 56. FAO, Rome. Available from: <https://www.fao.org/3/X0490E/x0490e00.htm>
- Amadori M, Morini G, Piccolroaz S, Toffolon M, 2020. Involving citizens in hydrodynamic research: A combined local knowledge-numerical experiment on Lake Garda, Italy. *Sci Total Environ* 722:137720.
- Balistrocchi M, Tomirotti M, Muraca A, Ranzi R, 2021. Hydroclimatic Variability and Land Cover Transformations in the Central Italian Alps. *Water* 13:963.
- Baracchini T, Wüest A, Bouffard D, 2020. Meteolakes: An operational online three-dimensional forecasting platform for lake hydrodynamics. *Water Res* 172:115529.
- Baroni C, Carton A, 1990 [Variazioni oloceniche della Vedretta della Lobbia (Gruppo dell'Adamello Alpi Centrali)]. [Article in Italian]. *Geogr Fis Din Quat* 13: 05-119.
- Berbenni P, Bertelli P, Occhi R, Bottazzi S, 1992. [Usi plurimi delle acque del Garda. La disciplina dei livelli del lago]. [Book in Italian]. Verona: Consorzio Universitario di Economia Industriale e Manageriale.
- Birhanu D, Kim H, Jang C, Park S, 2018. Does the complexity of evapotranspiration and hydrological models enhance robustness? *Sustainability* 10:2837.
- Brugnara Y, Brunetti M, Maugeri M, Nanni T, Simolo C, 2012. High-resolution analysis of daily precipitation trends in the central alps over the last century. *Int J Climatol* 32:1406-1422.
- Brugnara Y, Maugeri M, 2019. Daily precipitation variability in the southern alps since the late 19th century. *Int J Climatol* 39:3492-3504.
- Budyko MI, 1958. The heat balance of the earth's surface. Washington: US Dept. of Commerce, Weather Bureau: 259 pp.
- Budyko MI, 1974. Climate and life. New York, Academic Press: 508 pp.
- Calmanti S, Motta L, Turco M, Provenzale A, 2007. Impact of climate variability on Alpine glaciers in northwestern Italy. *Int J Climatol* 27:2041-2053
- Carolli M, Gelmini F, Pellegrini S, Deriu M, Zolezzi G, 2021. Prioritizing reaches for restoration in a regulated alpine river: Locally driven versus hydro-morphologically based actions. *River Res Appl* 37:17-32.
- Chebud YA, Melesse AM, 2009. Modelling lake stage and water balance of Lake Tana, Ethiopia. *Hydrol Process* 23:3534-3544.
- Cui J, Tian L, Gibson JJ, 2018. When to conduct an isotopic survey for lake water balance evaluation in highly seasonal climates. *Hydrol Process* 32:379-387.
- Dalton J, 1802. Experimental essays on the constitution of mixes gases: on the force of steam or vapor from water or other liquids in different temperatures, both in a Torricelli vacuum and in air; on evaporation; and on expansion of gases by heat. *Mem Lit Philos Soc Manchester* 5:536-602.
- De Marchi G, 1919. [Il regime idraulico del Lago di Garda]. [in Italian]. Venezia: Ufficio Idrografico del R. Magistrato alle Acque.
- De Marchi G, 1920. [Sul regime idraulico dei laghi ed in particolare di quello del Garda]. [Article in Italian]. *Giornale Genio Civile* 43.
- Do HX, Smith JP, Fry LM, Gronewold AD, 2020. Seventy-year long record of monthly water balance estimates for earth's largest lake system. *Sci Data* 7:1-12.
- Efstratiadis A, Koutsoyiannis D, 2010. One decade of multi-objective calibration approaches in hydrological modelling: a review. *Hydrol Sci J* 55:58-78.
- Elsawwaf M, Willems P, Feyen J, 2010. Assessment of the sensitivity and prediction uncertainty of evaporation models applied to Nasser Lake, Egypt. *J Hydrol* 395:10-22.
- European Centre for Medium-Range Weather Forecasts, 2014. Era-20c project (ECMWF atmospheric reanalysis of the 20<sup>th</sup> century) (Updated daily). Available from: <https://rda.ucar.edu/datasets/ds626.0/>
- Fink G, Schmid M, Wahl B, Wolf T, Wüest A, 2014. Heat flux modifications related to climate-induced warming of large European lakes. *Water Resour Res* 50:2072-2085.
- Fowe T, Karambiri H, Paturol JE, Poussin JC, Cecchi P, 2015. Water balance of small reservoirs in the Volta Basin: A case study of Boura reservoir in Burkina Faso. *Agric Water Manag* 152:99-109.
- Fuchs R, Herold M, Verburg PH, Clevers JG, 2013. A high-resolution and harmonized model approach for reconstructing and analyzing historic land changes in Europe. *Biogeosciences* 10:1543-1559.
- Fuchs R, Herold M, Verburg PH, Clevers JG, Eberle J, 2015. Gross changes in reconstructions of historic land cover/use for Europe between 1900 and 2010. *Global Change Biol* 21:299-313.
- Gibson J, Edwards T, 2002. Regional water balance trends and evaporation-transpiration partitioning from a stable isotope survey of lakes in Northern Canada. *Global Biogeochem Cycles* 16:10-1-10-14.
- Gibson J, Prowse T, Peters D, 2006. Hydroclimatic controls on water balance and water level variability in Great Slave Lake. *Hydrological Processes* 20:4155-4172.
- Goffi G, Osti L, Nava CR, Maurer O, Pencarelli T, 2021. Is preservation the key to quality and tourists' satisfaction? Evidence from Lake Garda. *Tour Recreat Res* 46:434-440.

- Golub M, Thiery W, Marcé R, Pierson D, Vanderkelen I, Mercado D, et al., 2022. A framework for ensemble modelling of climate change impacts on lakes worldwide: the Isimip Lake sector. *Geosci Model Dev Discuss* 2022:1-57.
- Goovaerts P, 1997. *Geostatistics for natural resources evaluation*. Oxford, Oxford University Press: 483 pp.
- Gronewold AD, Smith JP, Read LK, Crooks JL, 2020. Reconciling the water balance of large lake systems. *Adv Water Resour* 137:103505.
- Guo M, Wu W, Zhou X, Chen Y, Li J, 2015. Investigation of the dramatic changes in lake level of the Bosten Lake in Northwestern China. *Theor Appl Climatol* 119:341-351.
- Hamon RW, Weiss LL, Wilson WT, 1954. Insolation as an empirical function of daily sunshine duration. *Mon Weather Rev* 82:141-146.
- Hargreaves GH, Samani ZA, 1985. Reference crop evapotranspiration from temperature. *Appl Eng Agric* 1:96-99.
- Hinegk L, Adami L, Zolezzi G, Tubino M, 2022. Implications of water resources management on the long-term regime of Lake Garda (Italy). *J Environ Manage* 301:113893.
- Hood JL, Roy JW, Hayashi M, 2006. Importance of groundwater in the water balance of an alpine headwater lake. *Geophys Res Lett* 33:L13405.
- Jensen ME, Haise HR, 1963. Estimating evapotranspiration from solar radiation. *J Irrig Drain Div* 89:15-41.
- Jeppesen E, Kronvang B, Meerhoff M, Søndergaard M, Hansen KM, Andersen HE, et al., 2009. Climate change effects on runoff, catchment phosphorus loading and lake ecological state, and potential adaptations. *J Environ Qual* 38:1930-1941.
- Jiang L, Nielsen K, Andersen OB, Bauer-Gottwein P, 2017. Monitoring recent lake level variations on the Tibetan Plateau using Cryosat-2 Sarin mode data. *J Hydrol* 544:109-124.
- Kampf SK, Burges SJ, Hammond JC, Bhaskar A, Covino TP, Eurich A, et al., 2020. The case for an open water balance: Re-envisioning network design and data analysis for a complex, uncertain world. *Water Resour Res* 56: e2019WR026699.
- Laiti L, Mallucci S, Piccolroaz S, Bellin A, Zardi D, Fiori A, et al., 2018. Testing the hydrological coherence of high-resolution gridded precipitation and temperature data sets. *Water Resour Res* 54:1999-2016.
- Lenters JD, Kratz TK, Bowser CJ, 2005. Effects of climate variability on lake evaporation: Results from a long-term energy budget study of Sparkling Lake, Northern Wisconsin (USA). *J Hydrol* 308:168-195.
- Lerman A, Hull A, 1987. Background aspects of lake restoration: water balance, heavy metal content, phosphorus homeostasis. *Swiss J Hydrol* 49:148-169.
- Li XY, Xu HY, Sun YL, Zhang DS, Yang ZP, 2007. Lake-level change and water balance analysis at Lake Qinghai, West China during recent decades. *Water Resour Manage* 21:1505-1516.
- Longinelli A, Stenni B, Genoni L, Flora O, Defrancesco C, Pellegrini G, 2008. A stable isotope study of the Garda Lake, Northern Italy: Its hydrological balance. *J Hydrol* 360:103-116.
- Lowe LD, Webb JA, Nathan RJ, Etchells T, Malano HM, 2009. Evaporation from water supply reservoirs: An assessment of uncertainty. *J Hydrol* 376:261-274.
- Lu J, Sun G, McNulty SG, Amatya DM, 2005. A comparison of six potential evapotranspiration methods for regional use in the Southeastern United States 1. *JAWRA J Am Water Resour Assoc* 41:621-633.
- Majidi M, Alizadeh A, Farid A, Vazifedoust M, 2015. Estimating evaporation from lakes and reservoirs under limited data condition in a semi-arid region. *Water Resour Manage* 29:3711-3733.
- Mallucci S, Majone B, Bellin A, 2019. Detection and attribution of hydrological changes in a large alpine river basin. *J Hydrol* 575:1214-1229.
- Martin JL, McCutcheon SC, Schottman RW, 2018. *Hydrodynamics and transport for water quality modeling*. Boca Raton, CRC Press: 816 pp.
- Martinelli J, 1881. [Del Lago di Garda e del suo emissario il Mincio]. [Book in Italian]. Mantova, Prem Stab Tipografico Mondovi.
- Matheron G, 1963. Principles of geostatistics. *Econ Geol* 58:1246-1266.
- Matta E, Amadori M, Free G, Giardino C, Bresciani M, 2022. A satellite-based tool for mapping evaporation in inland water bodies: Formulation, application, and operational aspects. *Remote Sens* 14:2636.
- McMahon T, Peel M, Lowe L, Srikanthan R, McVicar T, 2013. Estimating actual, potential, reference crop and pan evaporation using standard meteorological data: a pragmatic synthesis. *Hydrol Earth Syst Sci* 17:1331-1363.
- Ministero dei Lavori Pubblici, Servizio Idrografico, 1917. [Annali idrologici - parte prima e seconda]. [in Italian] Annali Idrologici 1.
- Mohebzadeh H, Fallah M, 2019. Quantitative analysis of water balance components in Lake Urmia, Iran using remote sensing technology. *Remote Sens Appl Soc Environ* 13: 389-400.
- Moore TN, Mesman JP, Ladwig R, Feldbauer J, Olsson F, Pilla RM, et al., 2021. Lakeensemblr: An R package that facilitates ensemble modelling of lakes. *Environ Model Softw* 143:105101.
- Penman HL, 1948. Natural evaporation from open water, bare soil and grass. *Proc R Soc Lond A Math Phys Sci* 193:120-145.
- Piccolroaz S, 2016. Prediction of lake surface temperature using the air2water model: guidelines, challenges, and future perspectives. *Adv Oceanogr Limnol* 7:5791.
- Piccolroaz S, Healey N, Lenters J, Schladow S, Hook S, Sahoo G, Toffolon M, 2018. On the predictability of lake surface temperature using air temperature in a changing climate: A case study for Lake Tahoe (USA). *Limnol Oceanogr* 63:243-261.
- Piccolroaz S, Majone B, Palmieri F, Cassiani G, Bellin A, 2015. On the use of spatially distributed, time-lapse microgravity surveys to inform hydrological modeling. *Water Resour Res* 51:7270-7288.
- Piccolroaz S, Toffolon M, Majone B, 2013. A simple lumped model to convert air temperature into surface water temperature in lakes. *Hydrol Earth Syst Sci* 17:3323-3338.
- Piccolroaz S, Woolway RI, Merchant CJ, 2020. Global reconstruction of twentieth-century lake surface water temperature reveals different warming trends depending on the climatic zone. *Clim Change* 160:427-442.
- Priestley CHB, Taylor RJ, 1972. On the assessment of surface heat flux and evaporation using large-scale parameters. *Mon Weather Rev* 100: 81-92.
- Provincia Autonoma di Trento, 2006. [Piano Generale di Utilizzazione delle Acque Pubbliche]. [in Italian]. Available from: <http://pguap.provincia.tn.it/>
- Ranzi R, Grossi G, Gitti A, Taschner S, 2010. Energy and mass balance of the Mandrone glacier (Adamello, central Alps). *Geogr Fis Dinam Quat* 33:45-60.

- Ranzi R, Caronna P, Tomirotti M, 2017. Impact of climatic and land use changes on river flows in the Southern Alps, p. 61-83. In: E Kolokytha, S Oishi and RSV Teegavarapu (eds.), Sustainable water resources planning and management under climate change. Singapore, Springer.
- Ranzi R, Michailidi E, Tomirotti M, Crespi A, Brunetti M, Maugeri M, 2021. A multi-century meteorological analysis for the Adda river basin (Central Alps). Part II: Daily runoff (1845-2016) at different scales, *Int J Climatol* 41:181-199.
- Ravazzani G, Corbari C, Morella S, Gianoli P, Mancini M, 2012. Modified Hargreaves-Samani equation for the assessment of reference evapotranspiration in Alpine river basins. *J Irrig Drain Eng* 138:592-599.
- Rimmer A, Samuels R, Lechinsky Y, 2009. A comprehensive study across methods and time scales to estimate surface fluxes from Lake Kinneret, Israel. *J Hydrol* 379:181-192.
- Rosenberry DO, Winter TC, Buso DC, Likens GE, 2007. Comparison of 15 evaporation methods applied to a small mountain lake in the Northeastern USA. *J Hydrol* 340:149-166.
- Santilli M, Orombelli G, Pelfini M, 2002. Variations of Italian glaciers between 1980 and 1999 inferred by the data supplied by the Italian Glaciological Committee. *Geograf Fis Din Quat* 25:61-76.
- Safeeq M, Bart RR, Pelak NF, Singh CK, Dralle DN, Hartsough P, Wagenbrenner JW, 2021. How realistic are water-balance closure assumptions? A demonstration from the Southern Sierra Critical Zone observatory and Kings River experimental watersheds. *Hydrol Process* 35:e14199.
- Salmaso N, Mosello R, 2010. Limnological research in the deep southern subalpine lakes: synthesis, directions and perspectives. *Adv Oceanogr Limnol* 1:2594.
- Scavia D, DePinto JV, Bertani I, 2016. A multi-model approach to evaluating target phosphorus loads for Lake Erie. *J Great Lakes Res* 42:1139-1150.
- Schulz S, Darehshouri S, Hassanzadeh E, Tajrishy M, Schüth C, 2020. Climate change or irrigated agriculture - what drives the water level decline of Lake Urmia. *Sci Rep* 10:1-10.
- Sen PK, 1968. Estimates of the regression coefficient based on Kendall's tau. *J Am Stat Assoc* 63:1379-1389.
- Swenson S, Wahr J, 2009. Monitoring the water balance of Lake Victoria, East Africa, from space. *J Hydrol* 370:163-176.
- Szesztay K, 1974. Water balance and water level fluctuations of lakes. *Hydrol Sci J* 19:73-84.
- Theil H, 1950. A rank-invariant method of linear and polynomial regression analysis. *Ind Math* 1:467-482.
- Tian L, Liu Z, Gong T, Yin C, Yu W, Yao T, 2008. Isotopic variation in the lake water balance at the Yamdruk-Tso Basin, southern Tibetan plateau. *Hydrol Process* 22:3386-3392.
- Toffolon N, Piccolroaz S, Majone B, Soja AM, Peeters F, Schmid M, Wüest A, 2014. Prediction of surface temperature in lakes with different morphology using air temperature. *Limnol Oceanogr* 59:2182-2202.
- Togliani C, 2014. [La civiltà del fiume: Mincio paesaggio complesso. La civiltà del fiume]. [Book in Italian]. Milan, Franco Angeli Ed.: 240 pp
- Tolotti M, Dubois N, Milan M, Perga ME, Straile D, Lami A, 2018. Large and deep perialpine lakes: a paleolimnological perspective for the advance of ecosystem science. *Hydrobiologia* 824:291-321.
- Turner KW, Wolfe BB, Edwards TW, 2010. Characterizing the role of hydrological processes on lake water balances in the Old Crow Flats, Yukon Territory, Canada, using water isotope tracers. *J Hydrol* 386:103-117.
- Valiantzas JD, 2006. Simplified versions for the Penman evaporation equation using routine weather data. *J Hydrol* 331:690-702.
- Voinov A, Kolagani N, McCall MK, Glynn PD, Kragt ME, Ostermann FO, et al., 2016. Modelling with stakeholders - next generation. *Environ Model Softw* 77:196-220.
- Wale A, Rientjes T, Gieske A, Getachew H, 2009. Ungauged catchment contributions to Lake Tana's water balance. *Hydrol Process* 23:3682-3693.
- Winkler K, Fuchs R, Rounsevell M, Herold M, 2021. Global land use changes are four times greater than previously estimated. *Nat Commun* 12:1-10.
- Winkler K, Fuchs R, Rounsevell MDA, Herold M, 2020. HILDA+ Global Land Use Change between 1960 and 2019. PANGAEA. Available from: <https://doi.pangaea.de/10.1594/PANGAEA.921846>
- Winter TC, 1981. Uncertainties in estimating the water balance of lakes I. *JAWRA J Am Water Resour Assoc* 17:82-115.
- Winter TC, Buso DC, Rosenberry DO, Likens GE, Sturrock AJM, Mau DP, 2003. Evaporation determined by the energy-budget method for Mirror Lake, New Hampshire. *Limnol Oceanogr* 48: 995-1009.
- Yin X, Nicholson SE, 1998. The water balance of Lake Victoria. *Hydrol Sci J* 43:789-811.
- Zhang L, Potter N, Hickel K, Zhang Y, Shao Q, 2008. Water balance modeling over variable time scales based on the Budyko framework - model development and testing. *J Hydrol* 360:117-131.
- Zhao L, Xia J, Xu CY, Wang Z, Sobkowiak L, Long C, 2013. Evapotranspiration estimation methods in hydrological models. *J Geogr Sci* 23:359-369.
- Zhou S, Kang S, Chen F, Joswiak DR, 2013. Water balance observations reveal significant subsurface water seepage from Lake Nam Co, South-Central Tibetan Plateau. *J Hydrol* 491:89-99.
- Zorzin R, Tottola F, 2020. [Monte Baldo veronese: appunti di idrogeologia e carsismo]. [Article in Italian]. *Boll Museo Civ Storia Nat Verona* 44:27-51.

*Online supplementary material:*

*Review all the formulas used in this work*

*Fig. S1. Mount Baldo catchment contribution.*

*Fig. S2. Power-law curves for Lake Garda.*

*Fig. S3. Lake Garda climatological cycles.*

*Fig. S4. Digital Terrain Model of the Garda catchment.*

*Fig. S5. HILDA+ LULC categories within the Lake Garda catchment.*